Modeling the Phase Partitioning Behavior of Gas Tracers Under Geothermal Reservoir Conditions

Mark Trew[†]
Michael O'Sullivan
Department of Engineering Science, University of Auckland, New Zealand

Yoshio Yasuda
JAPEX Research Center, Japan

Abstract

A model of the liquid-vapor phase partitioning behavior of low concentrations of gas tracers in water at geothermal temperatures and pressures is presented. This model uses Henry's coefficient to describe the variation of the gas tracer solubility with temperature and pressure. A new method is described for the determination and representation of Henry's coefficients. The method uses experimentally determined values of Henry's coefficient and a theoretically predicted value of behavior at the critical point of water to provide data which can be fitted by a semi-empirical correlation. No assumptions regarding ideal behavior are necessary. The semi-empirical correlation is a modified version of that presented by Harvey (1996) and better accounts for high temperature and non-ideal behavior. Sets of model coefficients are given for a range of possible gas tracers. The resulting phase partitioning model is simple and may be easily implemented in a numerical geothermal simulator. The use and behavior of the model is illustrated by its application to a number of idealised test problems.

Keywords: Henry's law coefficient; Phase partitioning; Fugacity; Ideal gas; Peng-Robinson equation of state; Correlation.

1. Introduction

Computer modelling of flows including geothermal tracers is motivated by the widespread use of tracers in geothermal reservoir testing and management. These tracer models are useful for both the design and interpretation of field tests. The tracers used in geothermal fields may be broadly categorised into gas tracers and liquid tracers. Gas tracers are defined as those tracer chemicals that are highly volatile, sparingly soluble in the liquid phase and are injected as a vapor. Examples of gas tracers include the noble gases, refrigerants (e.g. R-23) and sulfur hexafluoride (SF_6). Liquid tracers have low or moderate volatility and may be injected as liquids. Examples include tritiated water, salt solutions (e.g. NaBr) and various alcohols (e.g. methanol). Liquid tracers may exhibit liquid-vapor phase partitioning behavior similar or quite different to that of the geothermal water. As discussed in Trew et al. (2000), distinctive models

[†]Corresponding author. Email: m.trew@auckland.ac.nz

of phase partitioning behavior are required for each of these two tracer categories. This paper describes recent advances in models of the phase partitioning behavior of gas tracers.

The description of the liquid-vapor phase partitioning of gas tracers is based on their solubility in water. Gas solubility data in water at low temperatures are relatively abundant. However, they are scarce for the higher temperatures encountered in geothermal reservoirs (Schotte 1985, Japas and Levelt Sengers 1989). Suitable methods for extrapolating low temperature solubility data or relationships to high temperatures must be considered. In this research only gas tracers that are sparingly soluble are considered and, hence, the gas tracer is close to infinite dilution in the liquid phase and its liquid-vapor partitioning behavior can be modelled by Henry's law (Schotte 1985). Henry's law has been used often in geothermal applications where gases are present; for example: O'Sullivan et al. (1985), Mroczek (1997) and Pruess et al. (2000). Henry's law requires the specification of Henry's coefficient which accounts for the solubility of the gas tracer in water varying with temperature and perhaps pressure. The representation of this coefficient is the key modeling consideration.

A geothermal flow simulator usually requires that a liquid-vapor phase partitioning model provide the liquid and vapor phase mass fractions of tracer for a given set of temperature and pressure conditions. Trew et al. (2000) describe the calculations required to implement a liquid-vapor partitioning model for gas tracers in the widely used TOUGH2 geothermal simulator program (Pruess 1991, Pruess et al. 1999). In developing the phase partitioning model described in Trew et al. (2000) it was assumed that gas behavior was ideal and that the concentration of gas tracers in both the liquid and vapor phases was very small. Consequently, given a temperature, T, and a partial gas pressure, P_g, the mass fractions of tracer in the liquid phase, X_g, and in the vapor phase, Y_g, were calculated as:

$$X_g = \frac{P_g}{C_H(T)} \frac{M_g}{M_{\mathrm{H_2O}}} \tag{1}$$

$$Y_g = \frac{\rho_g(P_g, T)}{\rho_s(T)} \tag{2}$$

where $C_H(T)$ is Henry's coefficient as a function of temperature, M_g is the molecular weight of the gas, $M_{\mathrm{H_2O}}$ is the molecular weight of water, ρ_g is the density of the gas and ρ_s is the density of steam. The gas density was calculated using an ideal gas law. The value of Henry's coefficient is more strongly temperature dependent than pressure dependent. In most cases a standard, or reference, pressure state of water vapor pressure is adopted and the coefficient is given at the standard state pressure.

In Trew et al. (2000) the temperature dependence of C_H was represented by fitting discrete C_H values at a range of temperatures by the Harvey (1996) correlation. The Harvey correlation is attractive for its simplicity and only contains three unknown parameters that must be determined from experimental data. The discrete C_H values were determined for a given temperature, T, from regressions of the gas distribution coefficients, β (it was assumed that $\beta = Y_g/X_g$), by using:

$$C_H(T) = \frac{\beta(T) R T_a \rho_s}{M_{\mathrm{H_2O}}} \tag{3}$$

where R is the universal gas constant and T_a is the absolute temperature. The gas distribution coefficients were obtained from low temperature (i.e. $20^\circ\mathrm{C}$ to $80^\circ\mathrm{C}$) regressions provided by Adams (pers. comm. 1999). These regressions were based on published data for various gases from Wilhelm et al. (1977) and Wen and Muccitelli (1979) and unpublished data from DuPont for the refrigerant gas R-134a.

The gas tracer phase partitioning model described above and used by Trew et al. (2000) was easy to implement because of its simplicity. However, there were a number of limitations to the model, including: the assumption of ideal gas behavior; the assumption of very small gas concentrations in all phases; the uncertain extrapolation of low temperature relationships to geothermal temperatures; no accounting for pressure effects in the specification of Henry's coefficient; and occasional problems with the Harvey correlation of the C_H values for some gas tracers. These limitations are addressed in this paper.

A phase partitioning model is presented which contains some similarities to that of Trew et al. (2000). However, the model described in this paper calculates mole fractions first and then converts them to mass fractions and most significantly uses a modified definition of Henry's coefficient that includes the effects of non-ideal behavior and pressure dependence.

The experimental calculation and semi-empirical fitting of this modified form of Henry's coefficient are the principal focus of this paper. The determination and use of this coefficient does not assume ideal gas behavior and incorporates the theoretical behavior of Henry's coefficients at the critical point of water. A modified form of the semi-empirical Harvey (1996) correlation for Henry's coefficient is proposed that retains the simplicity of the original form but has improved fitting characteristics. The final expression given for Henry's coefficient correlates not only temperature effects, but also pressure effects. The necessary correlation coefficients are determined for a selection of gas tracers and finally some applications are presented.

The effects of geothermal brine salinity on the phase partitioning behavior of gas tracers is beyond the scope of this research. In general it is expected that the solubility of the gas tracers in the liquid phase will decrease with increasing electrolyte concentration (Walas 1985, Hermann et al. 1995, Smits et al. 1998, Gao et al. 1999).

2. A Liquid-Vapor Phase Partitioning Model for Multiple Gas Tracers in Water

A liquid-vapor phase partitioning model that can be used in a geothermal flow simulator will generally provide expressions for the liquid and vapor phase mass fractions of gas tracer. However, the calculations are most easily performed to determine mole fractions with the mole fractions of tracer in each phase subsequently converted into mass fractions.

Consider a system with N gas tracers and water. Given a low solubility, Henry's law (Van Ness and Abbott 1997) can be used for tracer i to relate the liquid mole fraction, x_i, to the vapor phase mole fraction, y_i, the temperature, T, and the pressure, P, as:

$$x_i = \frac{y_i P}{C_H^*(T,P)_i}. \tag{4}$$

where $C_H^*(T,P)_i$ is a modified Henry's coefficient for tracer i that includes non-ideal behavior and accounts for the liquid phase solubility varying with temperature and pressure. The vapor mole fraction and the pressure can be conveniently combined into a single variable: $P_{g_i} = y_i P$. This variable is identical to the partial pressure of an ideal gas component from Dalton's law of partial pressures. Thus, if the partial pressure is used as a dependent variable along with temperature and pressure, the liquid and vapor mole fractions of the gas tracer i are determined from:

$$x_i = \frac{P_{g_i}}{C_H^*(T,P)_i} \tag{5}$$

$$y_i = \frac{P_{g_i}}{P}. \tag{6}$$

Once the values of x and y have been determined for the N tracers, the liquid and vapor phase water mole fractions are:

$$x_w = 1 \quad \sum_{i=1}^{N} x_i \tag{7}$$

$$y_w = 1 \quad \sum_{i=1}^{N} y_i. \tag{8}$$

The mass fraction values that are necessary for modelling the phase partitioning of the gas tracer are calculated as:

$$X_i = \frac{x_i M_i}{x_w M_w + \sum_{j=1}^{N} x_j M_j} \tag{9}$$

$$Y_i = \frac{y_i M_i}{y_w M_w + \sum_{j=1}^{N} y_j M_j}. \tag{10}$$

where M is the molecular weight, X is the liquid phase mass fraction and Y is the vapor phase mass fraction. The use of these mass fractions in the TOUGH2 geothermal simulator (Pruess 1991, Pruess et al. 1999) has been described in Trew et al. (2000). The key to this phase partitioning model is the modified Henry's coefficient which is discussed in the following sections.

3. Experimental Calculation and Fitting of a Modified Henry's Coefficient

3.1. Henry's law and a modified form of Henry's coefficient

This section shows how a modified form of Henry's coefficient can be obtained from experimental data and used with Henry's law to calculate liquid mole fractions of gas tracer in water for a general temperature and pressure state. No assumption of ideal behavior is made. The only assumption is that the solubility and, hence, liquid phase concentration of the gas tracer is sufficiently small so as to be approximately infinitely dilute.

To account for a non-ideal component i in a non-ideal mixture, the quantities of fugacity, f, and the partial fugacity of component i, $\hat{f}_i$, are necessary. The fugacity may be either that of the mixture or that of the pure component i, i.e. f_i. The fugacity and partial fugacity are defined as those quantities that replace pressure and partial pressure in the ideal pressure, temperature and molar volume relationships in order to maintain the validity of these relationships for non-ideal components and mixtures (Walas 1985). When multiple phases are present, the partial fugacities of component i in the liquid and vapor phases become equal when the vapor and liquid phases are in equilibrium (Van Ness and Abbott 1997), i.e.:

$$\hat{f}_i^v = \hat{f}_i^l = \hat{f}_i. \tag{11}$$

Henry's law is based on the relationship between the gas tracer partial liquid fugacity and its liquid mole fraction, x. This is shown in Figure 1. Henry's law defines a hypothetical linear liquid phase partial fugacity and liquid mole fraction relationship for the gas tracer which corresponds to the true state at infinite liquid dilution of the gas tracer (Benson and Krause 1989). The slope of this relationship is the value of Henry's coefficient, C_H. The formal definition of Henry's coefficient is (Benson and Krause 1989, Van Ness and Abbott 1997):

$$C_H = \lim_{x \to 0} \frac{\hat{f}_g^l}{x} \tag{12}$$

where $\hat{f}_g^l$ is the partial fugacity of the gas tracer in the liquid phase.

Although Henry's coefficient is temperature and pressure dependent it is usually given at a standard pressure state of water vapor pressure. Pressure dependence is recovered by using a Poynting correction factor (PCF) to reference the standard state Henry's coefficient at the water vapor pressure, $C_H(T, P_w^s)$, to the general pressure state, $C_H(T, P)$ (Benson and Krause 1989):

$$C_H(T,P) = C_H(T,P_w^s)\exp\left[\frac{\hat{V}_g^l(P \quad P_w^s)}{RT_a}\right] \tag{13}$$

where $\hat{V}_g^l$ is the partial liquid molar volume at infinite dilution and the standard pressure state, R is the universal gas constant and T_a is the absolute temperature. The PCF is determined by integrating an expression for the rate of change of fugacity with pressure, using the assumption that the partial liquid molar volume varies negligibly with pressure (Walas 1985, Benson and Krause 1989).

The vapor phase partial fugacity coefficient of the gas tracer, $\hat{\phi}_g^v$, is defined as (Van Ness and Abbott 1997):

$$\hat{\phi}_g^v = \frac{\hat{f}_g^v}{yP} \tag{14}$$

where $\hat{f}_g^v$ is the partial fugacity of the gas tracer in the vapor phase and y is the mole fraction of the gas tracer in the vapor phase. Rearrangement and division by the liquid phase mole fraction of tracer, x, gives:

$$\frac{\hat{f}_g^v}{x} = \frac{\hat{\phi}_g^v yP}{x} \tag{15}$$

Assuming that the solubility and mass of the gas tracer is sufficiently small so that it is approximately infinitely dilute in the liquid phase, (11), (12) and (15) may be used to give the pressure and temperature dependent Henry's coefficient as:

$$C_H(T,P) = \frac{\hat{\phi}_g^v yP}{x} \tag{16}$$

A Poynting correction factor can then be used to express the standard state Henry's coefficient as:

$$C_H(T,P_w^s) = \frac{\hat{\phi}_g^v yP}{x}\exp\left[\frac{\hat{V}_g^l(P \quad P_w^s)}{RT_a}\right] \tag{17}$$

Experimental gas solubility data are usually available for gas-solvent binary mixtures as the mole fraction of gas in the liquid solvent, x, at a given pressure, P and temperature, T. Equation (17) can be used to determine experimental values of C_H using T, P, and x, if y, $\hat{\phi}_g^v$ and $\hat{V}_g^l$ can be determined by auxiliary calculations. Section 3.2. describes the calculation of y and sections 3.4. and 3.5. describe the calculation of $\hat{\phi}_g^v$ and $\hat{V}_g^l$ and other quantities necessary to evaluate y. The experimentally derived values of $C_H(T, P_w^s)$ are fitted by a semi-empirical relationship which describes their variation with temperature.

When the semi-empirical relationship between $C_H(T, P_w^s)$ and temperature is defined, Henry's law is used to calculate the liquid mole fractions at a given temperature and pressure.

Equation (17) can be rearranged to:

$$x = \frac{P_g}{\frac{C_H(T)}{\hat{\phi}_g^v(T)}} \exp\left[\frac{\hat{V}_g^l(P \quad P_w^s)}{RT_a}\right] \tag{18}$$

where $P_g = yP$ is the partial gas pressure. This expression for x accounts for non-ideal behavior as well as temperature and pressure effects. It can be observed that if this equation is further rearranged to:

$$x = \frac{P_g}{C_H^*(T) \exp\left[\frac{\hat{V}_g^l(P \quad P_w^s)}{RT_a}\right]} \tag{19}$$

then the modified standard state Henry's coefficient, $C_H^*(T)$, implicitly contains the partial fugacity coefficient necessary to account for non-ideal behavior. Equation (19) is identical to (5). It is proposed then that the modified Henry's coefficient $C_H^* = C_H(T, P_w^s)/\hat{\phi}_g^v(T, P_w^s)$ rather then C_H be fitted using a semi-empirical fit. This approach has the attractive feature that once C_H^* is fitted, the partial fugacity coefficient does not need to be calculated every time the liquid mole fraction of the gas tracer, x, at a given temperature and pressure is required.

3.2. The vapor phase mole fraction of gas tracer

This section describes the derivation of the calculations required to determine the vapor phase mole fraction of gas tracer, y, given TPx experimental data. The derivation assumes that the experimental data are for a binary mixture of gas tracer and water and that the solubility and mass of the gas tracer are sufficiently small so as to be approximately infinitely dilute in the liquid phase. This means that the activity coefficient of the water component is very close to unity for all temperatures and does not need to be modelled (Fernandez-Prini and Crovetto 1985, Mroczek 1997). In order to take advantage of this, the expression for the vapor phase mole fraction of gas tracer is based on relationships involving the water component.

The liquid phase activity coefficient for water, γ_w, is defined as(Van Ness and Abbott 1997):

$$\gamma_w = \frac{\hat{f}_w^l}{x_w f_w} \tag{20}$$

The vapor phase partial fugacity coefficient, $\hat{\phi}_w^v$, is (Van Ness and Abbott 1997):

$$\hat{\phi}_w^v = \frac{\hat{f}_w^v}{y_w P} \tag{21}$$

where y_w is the vapor phase mole fraction of water. At equilibrium:

$$\hat{f}_w^l = \hat{f}_w^v \tag{22}$$

With rearrangement, and using the fact that the activity coefficient of water is one, the vapor phase mole fraction of water is:

$$y_w = \frac{x_w f_w}{\hat{\phi}_w^v P} \tag{23}$$

By definition the pure component fugacity at the standard pressure state, P_w^s, is: $f_w^s = \phi_w^s P_w^s$. The pure component fugacity of water may be referred to a general pressure state through the use of a PCF:

$$f_w = \phi_w^s P_w^s \exp\left[\frac{\hat{V}_w^l(P \quad P_w^s)}{RT_a}\right] \tag{24}$$

Assuming that x and y refer to the liquid and vapor mole fractions of gas tracer respectively, the expression relating the liquid mole fraction of gas tracer to the vapor mole fraction of gas tracer in a binary mixture with water at a given temperature is:

$$1 \quad y = \frac{\gamma_w(1 \quad x)\phi_w^s P_w^s}{\hat{\phi}_w^v P} \exp\left[\frac{\hat{V}_w^l(P \quad P_w^s)}{RT_a}\right] \tag{25}$$

An important feature of (25) is its non-linearity. The value of $\hat{\phi}_w^v$ also depends on the unknown vapor mole fraction of tracer y, therefore y must be determined iteratively. The calculations required for the auxiliary values: ϕ_w^s, $\hat{\phi}_w^v$ and $\hat{V}_w^l$; are described in sections 3.4. and 3.5..

3.3. Calculating the Henry coefficient, $C_H(T, P_w^s)$ when only β is known

For the gas tracers R-134a, R-124 and R-125 considered in this research, experimental TPx data were not available. However, regressions of the gas distribution coefficient, β, with temperature were provided by Adams (pers. comm. 1999). The gas distribution coefficient represents the distribution of the gas tracer between the liquid and vapor phases and is the ratio of the vapor phase concentration to the liquid phase concentration. If this ratio is expressed in units of molality, it can be rearranged to give a distribution ratio in terms of the vapor and liquid phase mole fractions of the gas tracer:

$$\beta = \frac{y(1 \quad x)}{x(1 \quad y)} \tag{26}$$

This ratio can be rearranged to give an expression for the liquid phase mole fraction of gas tracer:

$$x = \frac{y}{\beta + y(1 \quad \beta)} \tag{27}$$

The expression for x can be used together with:

$$1 \quad y = \frac{\gamma_w(1 \quad x)\phi_w^s P_w^s}{\hat{\phi}_w^v P} \exp\left[\frac{V_w^l(P \quad P_w^s)}{RT_a}\right] \tag{28}$$

to iteratively determine x and y values from β values derived at low temperatures from a β regression. The x and y values can then be used to determine the standard state Henry's coefficients using (17).

3.4. The Peng-Robinson equation of state

A relationship between the pressure, temperature and molar volume of a gas tracer and water mixture is necessary to determine successfully the auxiliary values ($\hat{\phi}_g^v$, $\hat{V}_g^l$, ϕ_w^s, $\hat{\phi}_w^v$ and $\hat{V}_w^l$) necessary for calculating y, C_H and C_H^*. One such relationship is the theoretical Peng-Robinson

equation of state (Peng and Robinson 1976). This equation of state has been widely used in chemical engineering applications, and was used by Mroczek (1997) in his experimental work with SF_6 at geothermal temperatures and pressures.

For a mixture, the Peng-Robinson equation of state (PREOS) (Peng and Robinson 1976) is:

$$P = \frac{RT_a}{V \quad b} \quad \frac{a(T_a)}{V(V+b)+b(V \quad b)} \tag{29}$$

where P is the mixture pressure, T_a is the absolute temperature, V is the mixture molar volume and a and b are mixture parameters depending on the pure component critical parameters (T_i^c, P_i^c), the acentric factor (w_i)* and the temperature. For component i in a multi-component mixture, a_i and b_i are defined as:

$$a_i(T) = 0.45724 \frac{R^2 T_i^{c2}}{P_i^c} \alpha(T_i^r, \omega_i) \tag{30}$$

$$b_i(T) = 0.07780 \frac{RT_{ci}}{P_{ci}} \tag{31}$$

where T_i^r is the temperature reduced by the critical temperature of component i, i.e. $T_i^r = T_a/T_i^c$.

A number of choices of the $\alpha(T_i^r, \omega_i)$ function have been presented in the literature (Peng and Robinson 1976, Tsai and Chen 1998), derived by fitting pure component vapor pressure values and finding the values of α such that the liquid and vapor phase fugacities match along the saturation curve. In this research a generalised α function given by Twu et al. (1995) has been used. The α function for each component is expanded as a power series in the acentric factor and the unknown functions fitted from vapor pressure values. The results are (Twu et al. 1995):

$$\alpha = \alpha^{(0)} + \omega \quad \alpha^{(1)} \quad \alpha^{(0)}\big) \tag{32}$$

$$T^r \leq 1 \begin{cases} \alpha^{(0)} = T^r \quad {}^{0.171813} e^{0.125283\left(1 \quad T^{r\,1.77634}\right)} \\ \alpha^{(1)} = T^r \quad {}^{0.607352} e^{0.511614\left(1 \quad T^{r\,2.20517}\right)} \end{cases} \tag{33}$$

$$T^r > 1 \begin{cases} \alpha^{(0)} = T^r \quad {}^{0.792615} e^{0.401219\left(1 \quad T^{r} \quad {}^{0.992615}\right)} \\ \alpha^{(1)} = T^r \quad {}^{1.98471} e^{0.024955\left(1 \quad T^{r} \quad {}^{9.98471}\right)} \end{cases} \tag{34}$$

The mixture values of a and b are (Peng and Robinson 1976):

$$a = \sum_i \sum_j z_i^k z_j^k a_{ij} \tag{35}$$

$$a_{ij} = (1 \quad \gamma_{ij}) \sqrt{a_i a_j} \tag{36}$$

$$b = \sum_i z_i^k b_i \tag{37}$$

where z_i^k is the mole fraction of component i in phase k of the mixture. The binary interaction component, γ_{ij}, characterises the binary formed by components i and j. Its value was set to 0.5 in this work, following Mroczek (1997). In addition to these original mixture rules for a and b given by Peng and Robinson (1976) other rules have been proposed, including those derived from combining Gibbs free energy models with an equation of state such as the PREOS (Fischer

*w_i was originally defined to represent the acentricity or nonsphericity of a molecule. At present it is used as a measure of the complexity of a molecule with respect to its geometry and polarity (Reid et al. 1977).

and Gmehling 1996, Dahl and Michelsen 1990, Gupte et al. 1986, Dahl et al. 1991, Larsen et al. 1987).

The PREOS may be expressed as a cubic equation in the mixture compressibility factor, Z:

$$Z^3 \quad (1 \quad B)Z^2 + (A \quad 3B^2 \quad 2B)Z \quad (AB \quad B^2 \quad B^3) = 0 \tag{38}$$

where:

$$A = \frac{a_m P}{R^2 T_a^2} \tag{39}$$

$$B = \frac{b_m P}{R T_a} \tag{40}$$

$$Z = \frac{PV}{R T_a}. \tag{41}$$

The real positive roots of this equation of the compressibilities of the current phase state. For example, in a two-phase state, the largest positive root is the vapor phase compressibility and the smallest positive root is the liquid phase compressibility. The partial fugacity coefficient for component i in phase k, necessary for further calculations, may be calculated as:

$$\ln \phi_i^k = \frac{b_i}{b}(Z^k \quad 1) \quad \ln (Z^k \quad B) \\ \frac{A}{2\sqrt{2}B}\left(\frac{2\sum_j z_j^k a_{ji}}{a} \quad \frac{b_i}{b}\right) \ln\left(\frac{Z^k + (1+\sqrt{2})B}{Z^k + (1 \quad \sqrt{2})B}\right) \tag{42}$$

3.5. Partial molar volumes

The partial molar volumes are necessary for the determination of the Poynting correction factors, i.e. pressure dependence, in the calculation of the vapor phase mole fraction and the standard state Henry coefficient. The molar volume of phase k of a mixture is related to the mixture compressibility for that phase (see Equation (41)) as:

$$V^k = \frac{Z^k R T}{P} \tag{43}$$

$$\Rightarrow \quad \frac{\partial V^k}{\partial z^k} = \frac{RT}{P}\frac{\partial Z^k}{\partial z^k} \tag{44}$$

where z^k is the mole fraction of gas tracer in phase k. For an N component mixture, the partial molar volume for component i is found from the mixture volume as (Walas 1985):

$$\hat{V}_i^k = V^k \quad \sum_{j \neq i}^{N} z_j^k \frac{\partial V^k}{\partial z_j^k} \tag{45}$$

For a binary mixture, if the liquid mole fraction of the gas tracer is x, then the water and gas component partial molar volumes in the liquid phase are:

$$\hat{V}_w^l = V^l \quad x\frac{\partial V^l}{\partial x} \tag{46}$$

$$\hat{V}_g^l = V^l + (1 \quad x)\frac{\partial V^l}{\partial x} \tag{47}$$

The mixture molar volume derivative with respect to the gas tracer mole fraction is found from Equation (44) and the PREOS cubic equation for the compressibility:

$$\frac{\partial}{\partial x}\left(Z^{l^3} \quad (1 \quad B)Z^{l^2} + \quad A \quad 3B^2 \quad 2B\right) Z^l \quad AB \quad B^2 \quad B^3)\Big) = 0 \tag{48}$$

$$\Rightarrow \quad \frac{\partial Z^l}{\partial x} = \frac{Z^{l^2}\frac{\partial B}{\partial x} \quad Z^l \quad \frac{\partial A}{\partial x} \quad 2(1+3B)\frac{\partial B}{\partial x}\big) + B\frac{\partial A}{\partial x} + (A \quad 2B \quad 3B^2)\,\frac{\partial B}{\partial x}}{\left(3Z^{l^2} \quad 2Z^l(1 \quad B) + A \quad 2B \quad 3B^2\right)} \tag{49}$$

To evaluate $\frac{\partial Z^l}{\partial x}$, the PREOS must be solved to find Z^l (the liquid phase root of the cubic PREOS), and mixture values for A, B, $\frac{\partial A}{\partial x}$ and $\frac{\partial B}{\partial x}$ are required. Using a single coefficient mixing rule (equations (35) to (37)) these mixture values are:

$$A = \frac{P}{R^2T^2} \quad (1 \quad x)^2 a_1 + 2x(1 \quad x)(1 \quad \gamma_{12})\sqrt{a_1 a_2} + x^2 a_2\big) \tag{50}$$

$$\Rightarrow \quad \frac{\partial A}{\partial x} = \frac{P}{R^2T^2}\,(\quad 2(1 \quad x)a_1 + 2(1 \quad 2x)(1 \quad \gamma_{12})\sqrt{a_1 a_2} + 2xa_2) \tag{51}$$

and

$$B = \frac{P}{RT}((1 \quad x)b_1 + xb_2) \tag{52}$$

$$\Rightarrow \quad \frac{\partial B}{\partial x} = \frac{P}{RT}(b_2 \quad b_1) \tag{53}$$

3.6. The modified Harvey correlation for Henry's coefficients

The Harvey semi-empirical correlation for Henry's coefficients (Harvey 1996, Harvey 1998) used by Trew et al. (2000) has the form:

$$\ln C_H = \ln P_w^s + \frac{A}{T_w^r} + B\frac{(1 \quad T_w^r)^{0.355}}{T_w^r} + C(T_w^r) \quad ^{0.41} e^{(1 \quad T_w^r)} \tag{54}$$

where A, B and C are correlation coefficients determined by fitting experimental data. This correlation was based on a number of previous works (Japas and Levelt Sengers 1989, Harvey and Levelt Sengers 1990) and was found to be effective for both interpolation and extrapolation of Henry's coefficients for a number of gases over a wide temperature range (Harvey 1996, Mroczek 1997, Harvey 1998).

The term $B(1 \quad T_w^r)^{0.355}/T_w^r$ is important as it correctly reproduces the divergent behavior of $\ln C_H$ at the solvent (water) critical point, i.e. (Schotte 1985):

$$\left.\frac{d\ln C_H}{dT}\right|_{T=T_w^c} = \quad \infty. \tag{55}$$

However, it is also known that at the solvent (water) critical point (Beutier and Renon 1978, Schotte 1985, Japas and Levelt Sengers 1989):

$$C_H(T_w^c, P_w^c) = \hat{\phi}_g^v(T_w^c, P_w^c)P_w^c \tag{56}$$

In this research it has been found through experimentation that the limiting value of C_H is not represented by the Harvey correlation in the form of (54), although the divergent behavior of $\ln C_H$ is correctly represented. To represent the limiting value, given in (56), it is necessary

that: $A + C = \ln \hat{\phi}_g^v(T_w^c, P_w^c)$. In practice, this constraint has been found to give a poor fit to the predominantly low temperature experimentally derived C_H values.

It can, however, be observed that if $C_H(T, P_w^s)/\hat{\phi}_g^v(T, P_w^s)$ is to be fitted by a correlation similar to that of Harvey (1996), then the final three terms must disappear as the solvent critical point is reached, i.e. $T_w^r \to 1$. A modified Harvey correlation (MHC) with these characteristics is proposed here:

$$\ln \frac{C_H}{\hat{\phi}_g^v(T, P_w^s)} = \ln P_w^s + A^* \frac{(1 \quad T_w^r)^{0.8}}{T_w^r} + B^* \frac{(1 \quad T_w^r)^{0.355}}{T_w^r} + C^*(1 \quad T_w^r)^{0.8}(T_w^r)^{\ 0.41} e^{(1 \ T_w^r)} \tag{57}$$

The MHC retains the simplicity of only three unknown coefficients, A^*, B^* and C^*, that must be fitted. The exponent of 0.8 has been arrived at by experimentation and gives good behavior. At the solvent critical point:

$$\ln C_H = \ln \hat{\phi}_g^v(T_w^c, P_w^c) + \ln P_w^c \tag{58}$$

as required.

3.7. An empirical correlation for the liquid phase partial molar volumes of gas tracers

As shown in (19), if pressure effects are to be included in the liquid-vapor partitioning model, then the partial molar gas volume at any given temperature is required to determine the Poynting correction factor. The calculations required for partial molar volumes given in Section 3.5. are overly cumbersome to use in an implementation of the partitioning model in a geothermal flow simulator. In addition, the effect of the Poynting correction factor is usually small. Therefore, it was decided to investigate a correlation for the liquid phase partial molar volumes in terms of temperature and molecular weight. A collection of gas tracers identical to those considered later in Section 4. (SF_6, R-13, R-14, R-22, R-23, R-116, R-C318, R-134a, R-124 and R-125) were used to develop the correlation.

Equation (47) was used to calculate the partial molar volumes of the gas tracers under consideration. The results over a temperature range from 0°C to approximately 370°C are shown in Figure 2(a). The expected behavior is seen. For example, the molar volume of SF_6 at its normal boiling point (-64°C) is estimated to be $0.73 \times 10^{\ -4} \mathrm{m}^3\mathrm{mol}^{\ -1}$ (Mroczek 1997), so a simple extrapolation suggests that the partial molar volumes for SF_6 derived from Equation (47) and the PREOS are quantitatively correct, at least at low temperatures. Furthermore, it has been shown that the partial molar volume of a gas solute diverges at the critical temperature of the solvent (Schotte 1985). So the partial molar volume behavior of the gas tracers is at least qualitatively correct at the critical point of water. A study of various infinite dilution partial molar volume models, including the PREOS, has shown that the models are only suitable for qualitative predictions around the solvent critical point (Liu and Macedo 1995).

The mean partial molar volumes for the 10 gas tracers under consideration have been sampled at a large number of temperature sample points and have been fitted by the non-linear empirical function:

$$\hat{V}_g^l(T_w^r) \approx \frac{6.7 \times 10^{\ -4} T_w^r + 8.1 \times 10^{\ -4}}{15(1 \quad T_w^r)^{1.28}} \tag{59}$$

This is shown in Figure 2(b).

The fit of the mean partial molar volumes by a function of T_w^r has been further moderated by a linear function of the molecular weight of the gas, M_g, to account for deviations from the mean values. The coefficients of the moderating function have been fitted to all the data in a least squares sense. The final form of the empirical partial molar volume function is:

$$\hat{V}_g^l(T_w^r, M_g) \approx (6.20 M_g + 0.34) \frac{6.7 \times 10^{\ 4} T_w^r + 8.1 \times 10^{\ 4}}{15(1 \quad T_w^r)^{1.28}} \tag{60}$$

This moderation provides improved representation at no extra cost of parameter specification.

The quality of the fit to the mean values and the molecular weight moderated fit is shown in Figure 3. In both plots, the fitted partial molar volumes are plotted against the values calculated using the Peng-Robinson equation of state. A perfect fit would lie along the diagonal line shown in Figure 3. Figure 3(a) clearly indicates that a significant improvement in the empirical correlation for these gas tracers has been achieved through the use of the molecular weight, at almost negligible extra computational expense. In particular, the fit is quite good up to 350°C. Figure 3(b) shows some interesting results for CO_2 and O_2. Although (59) was not determined using CO_2 or O_2, the final correlation (60) is good at predicting their partial molar volumes.

3.8. Summary of the steps required to fit the modified Henry's coefficients

This section presents an outline and summary of the steps required to determine the modified Harvey correlation coefficients.

1. As described in sections 3.2. to 3.5., experimental TPx or $TP\beta$ data are used to calculate $\hat{V}_w^l$, ϕ_w^v, y (and x if unknown), $\hat{V}_g^l$, $\hat{\phi}_w^v$ and $\hat{\phi}_g^v$. The calculation of y is non-linear as y and $\hat{\phi}_w^v$ are inter-dependent. These values are determined iteratively. The experimental values of Henry's coefficient at the standard state, $C_H(T, P_w^s)$, are determined from:

$$C_H^{\text{expt}}(T, P_w^s) = \frac{\hat{\phi}_g^v y P}{x} \exp\left[\frac{\hat{V}_g^l(P \quad P_w^s)}{RT_a}\right]. \tag{61}$$

2. Due to the sparsity of experimental data, it has been found best to scale $C_H^{\text{expt}}(T, P_w^s)$ by the partial fugacity coefficient of the gas tracer at the critical point and fit these values in a least squares sense by the modified Harvey correlation (MHC) described in Section 3.6.. The result of this fit is the intermediate quantity: $C_H^1(T, P_w^s)$.

3. The $C_H^1(T, P_w^s)$ function is evaluated for a number of temperatures from 0°C to 374°C and a modified Henry coefficient is calculated as:

$$C_H^{1\,*}(T, P_w^s) = \frac{C_H^1(T, P_w^s)}{\hat{\phi}_g^v(T, P_w^s)} \hat{\phi}_g^v(T_w^c, P_w^c). \tag{62}$$

4. In order to obtain a function for modeling purposes, the $C_H^{1\,*}(T, P_w^s)$ values are fitted in a least-squares sense using the MHC described in Section 3.6.. The resulting correlation gives $C_H^*(T, P_w^s)$ which is a standard state Henry's coefficient modified to account for non-ideality through the inclusion of the standard state fugacity coefficient.

5. The Poynting correction factor using the empirical correlation for the liquid phase partial molar volumes (Section 3.7.) is added to give a representation of a modified Henry's coefficient applicable to a general temperature and pressure state:

$$\ln C_H^*(T,P) = \ln P_w^s + A^* \frac{(1 \quad T_w^r)^{0.8}}{T_w^r} + B^* \frac{(1 \quad T_w^r)^{0.355}}{T_w^r} + C^*(1 \quad T_w^r)^{0.8}(T_w^r)^{\ 0.41} \exp(1 \quad T_w^r) + (6.20M_g + 0.34)\frac{(\ 6.7\times 10^{\ 4}T_w^r + 8.1\times 10^{\ 4})}{15(1 \quad T_w^r)^{1.28}T_w^c T_w^r}(P \quad P_w^s). \quad (63)$$

This is the modified Henry's coefficient which is used in (5) for calculating the gas tracer phase partitioning.

4. Modified Henry's Coefficients for a Selection of Gas Tracers

The selection of gases that have been specifically considered in this work are: SF_6, R-13, R-14, R-22, R-23, R-116, R-C318, R-134a, R-124 and R-125. Of these, R-23 and R-134a are currently used as tracers in The Geysers geothermal field (Adams pers. comm. 2001). R-13, R-22 and R-124 are listed as controlled substances by the Montreal Protocol (1987) and have a non-zero ozone-depletion potential, rendering them unacceptable as tracer chemicals. They have been included in this study for comparison purposes only. SF_6 has characteristics that may contribute to its relative lack of success as a tracer in vapor-dominated systems (Mroczek 1997, Adams pers. comm. 2001). However, extensive experimental SF_6 solubility data are available for a wide range of temperatures. This was useful for developing and testing the Henry's coefficient correlations.

The key properties of gas tracer considered here and the modified Harvey correlation coefficients resulting from the fitting process described in Section 3.8. are given in Table 1. Figure 4 compares the Harvey (1996) correlation of Henry's coefficients (as used in (Trew et al. 2000)) with the modified Harvey correlation for SF_6, R-134a and R-23. These examples illustrate that the improved theoretical foundations and empirical fitting process for Henry's coefficients presented in this research are clearly superior to those of (Trew et al. 2000) at the temperatures found in geothermal reservoirs.

Figures 5 to 14 show the temperature and pressure variations of the Henry coefficient correlations. Also shown is the available experimental data and the fit at each step in the process. The results indicate that non-ideal behavior becomes more significant for temperatures in excess of approximately 200°C. In addition, it can be observed that in general the variation in the modified Henry's coefficient with pressure from the standard state pressure is small. The exception to this is near the critical temperature of water where the partial molar volume of the gas tracer in mixture with water diverges (see Section 3.7.). It may be expected that for most practical simulations the pressure correction term in (63) is not necessary, however, given that it adds negligible computational overhead it can be retained for completeness.

5. Applications

5.1. Two-phase stream-tube flow

The comparative liquid and vapor partitioning behavior of gas tracers is best observed in a simple stream-tube test problem. The problem and its specifications are shown in Figure 15.

Fluid is injected with an enthalpy of 1.4×10^6 $\mathrm{J kg}^{-1}$, generating a two-phase flow regime. The steady-state pressure, vapor pressure, temperature and vapor saturation distributions are shown in Figure 16.

Three gas tracers are considered: SF_6, R-134a and R-23. The standard pressure state variations of Henry's coefficients with temperature for these tracers are given in Figure 4. This figure shows that at the temperatures considered in this problem (100°C to 300°C) the C_H values for SF_6 obtained using the modified Harvey correlation are similar to those of the Harvey (1996) correlation using the coefficients given in Trew et al. (2000). It is expected then that the phase partitioning model presented here and that of Trew et al. (2000) will give similar results since the key differences lie in the determination of Henry's coefficients.

The gas tracers are each injected at a rate of 0.1 $\mathrm{kg\,s}^{-1}$ for 20 minutes. The liquid and vapor phase tracer return curves at the production well are shown for the two-phase flow in Figures 17 to 19. Phase partitioning behavior calculated using the Harvey (1996) correlation of Henry's coefficients is compared to the model presented in this paper. The implementation of the partitioning models in TOUGH2 has been validated by comparison with known analytic solutions for single phase transport and convergence analysis for multiple phases.

As expected from the low gas tracer solubility, the production well concentrations of the gas tracers in the liquid phase are at least an order of magnitude less than those in the vapor phase. Figures 17(a) and 17(b) show the expected minor differences between partitioning behavior calculated using the Harvey (1996) correlation of Henry's coefficients and the modified Harvey correlation of this paper. The differences lie in the peak predicted tracer concentration and not in a time shift of the tracer pulse, thus suggesting that these arise due to the emergence of non-ideal behavior of the SF_6 tracer as the concentration increases. In the case of R-134a and R-23 gas tracers, the Harvey (1996) correlation of Henry's coefficients predicts lower solubilities at higher temperatures than those of the modified Harvey correlation and, particularly in the case of R-23, this is clearly erroneous behavior. Figures 17 to 19 show that the impact of the new models is to retard the breakthrough times of the gas tracers.

In the single phase region, Figure 16(a) shows that the difference $P \quad P_w^s$ varies from close to zero at the production to over 100 bar at the injection well. Although the value of $P \quad P_w^s$ is not negligible, its impact on the final results through the Poynting correction factor remains negligible and for most practical simulations the influence of pressure variations on the phase partitioning models may be neglected. However, given that its inclusion in the phase partitioning model presents negligible computational overhead, the term can be quite easily retained for completeness.

5.2. An idealised three-dimensional reservoir

The utility and value of gas tracer phase partitioning models coupled with a geothermal reservoir simulator is illustrated by the following problem. Steady-state two-phase convective flow is formed in an idealised reservoir of volume 1 km^3. The reservoir material is homogeneous with a porosity of 0.1 and a permeability of 10^{-14} m^2. The boundary blocks below the central column have a fixed internal energy of 1.85×10^4 $\mathrm{J kg}^{-1}$. The steady state temperature and vapor saturation iso-surfaces are shown in Figure 20. 100 kg of SF_6 is introduced into the center of the reservoir. The predicted transport over time of the gas tracer in the liquid and vapor phases is shown in Figure 21. The sparingly soluble SF_6 tracer is preferentially transported in the vapor phase, however, the flow is two-phase and local equilibrium exists between the phases at every point. Consequently, SF_6 is also detected in the liquid phase farther from the injection point than would be the case for a non-volatile tracer. For this example the cut-off

detection point has been nominally set to a mass fraction of 10^{-12}. This problem shows how models of tracer transport in geothermal reservoirs can be used as predictive and correlative tools to enhance both the design and the interpretation of field tracer tests.

6. Summary and Conclusions

A model of liquid-vapor phase partitioning of gas tracers in water at geothermal temperatures and pressures has been presented. The key feature of this model is the definition and determination of the Henry's coefficients that are used in Henry's law to model the liquid phase mole fraction of gas tracers. This coefficient has been derived from first principles and the assumption of ideal gas behavior has not been necessary. The definition of Henry's coefficient has been modified so that non-ideal behavior can be easily included in Henry's law. Experimental values of Henry's coefficient derived from solubility data have been fitted in two steps by a modified semi-empirical Harvey correlation that accounts for the theoretical behavior at the critical point of water. The semi-empirical correlation also accounts for pressures other than the vapor pressure of water, which is the standard state pressure. The new methods have been used to determine correlation coefficients for a range of gas tracers and the liquid-vapor phase partitioning models have been applied to some test problems.

The models and experimental reduction methods described in this research retain the simplicity and attractions of those presented in previous research by Trew et al. (2000). However, this new research has reduced levels of uncertainty in the process of determining the experimental values of Henry's coefficients and has proposed a new correlation of Henry's coefficients which is satisfactory for geothermal temperatures and pressures.

Acknowledgements

This study has been funded in part by the New Energy & Industrial Technology Development Organisation of Japan (NEDO). We also acknowledge the input of Mike Adams (EGI Utah), who provided gas solubility data and helpful comments.

References

Benson, B. and Krause, D., 1989. A Thermodynamic Treatment of Dilute Solutions of Gases in Liquids. Journal of Solution Chemistry 18(9), 803–821.

Beutier, D. and Renon, H., 1978. Gas solubilities near the solvent critical point. American Institute of Chemical Engineers Journal 24, 1122.

Dahl, S., Fredenslund, A. and Rasmussen, P., 1991. The MHV2 Model: A UNIFAC-Based Equation of State Model for Prediction of Gas Solubility and Vapor-Liquid Equilibria at Low and High Pressures. Industrial & Engineering Chemistry Research 30(8), 1936–1945.

Dahl, S. and Michelsen, M., 1990. High-Pressure Vapor-Liquid Equilibrium with a UNIFAC-Based Equation of State. American Institute of Chemical Engineers Journal 36(12), 1829–1836.

Fernandez-Prini, R. and Crovetto, R., 1985. A Critical Evaluation of the Solubility of Simple Inorganic Gases in Water at High Temperature. American Institute of Chemical Engineers Journal 31(3), 513–516.

Fischer, K. and Gmehling, J., 1996. Further development, status and results of the PSRK method for the prediction of vapor-liquid equilibria and gas solubilities. Fluid Phase Equilibria 121, 185–206.

Gao, G., Tan, Z. and Yu, Y., 1999. Calculation of high-pressure solubility of gas in aqueous electrolyte solution based on non-primitive mean spherical approximation and perturbation theory. Fluid Phase Equilibria 165, 169–182.

Gupte, P., Rasmussen, P. and Fredenslund, A., 1986. A New Group-Contribution Equation of State for Vapor-Liquid Equilibria. Industrial & Engineering Chemistry Fundamentals 25, 636–645.

Harvey, A., 1996. Semiempirical Correlation for Henry's Constants over Large Temperature Ranges. American Institute of Chemical Engineers Journal 42(5), 1491–1494.

Harvey, A., 1998. Applications of Near-Critical Dilute-Solution Thermodynamics. Industrial & Engineering Chemistry Research 37(8), 3080–3088.

Harvey, A. and Levelt Sengers, J., 1990. Correlation of Aqueous Henry's Constants from 0°C. American Institute of Chemical Engineers Journal 36(4), 539–546.

Hermann, C., Dewes, I. and Schumpe, A., 1995. The estimation of gas solubilities in salt solutions. Chemical Engineering Science 50(10), 1673–1675.

Japas, M. and Levelt Sengers, J., 1989. Gas Solubility and Henry's Law Near the Solvent's Critical Point. American Institute of Chemical Engineers Journal 35(5), 705–713.

Larsen, B., Rasmussen, P. and Fredenslund, A., 1987. A Modified UNIFAC Group-Contribution Model for the Prediction of Phase Equilibria and Heats of Mixing. Industrial & Engineering Chemistry Research 26, 2274–2286.

Liu, H. and Macedo, E., 1995. A Study on the Models for Infinite Dilution Partial Molar Volumes of Solutes in Supercritical Fluids. Industrial & Engineering Chemistry Research 34(6), 2029–2037.

Mroczek, E., 1997. Henry's Law Constants and Distribution Coefficients of Sulfur Hexafluoride in Water from 25 °C to 230 °C. Journal of Chemical and Engineering Data 42, 116–119.

O'Sullivan, M., Bodvarsson, G., Pruess, K. and Blakeley, M., 1985. Fluid and Heat Flow in Gas-Rich Geothermal Reservoirs. Society of Petroleum Engineers Journal 25(2), 215–226.

Peng, D. and Robinson, D., 1976. A new two-constant equation of state. Industrial & Engineering Chemistry Fundamentals 15(1), 59–64.

Pruess, K., 1991. TOUGH2 - A General Purpose Numerical Simulator for Multiphase Fluid and Heat Flow. Technical Report LBL-29400. Lawrence Berkeley Laboratory. Berkeley, California.

Pruess, K., Oldenburg, C. and Moridis, G., 1999. TOUGH2 User's Guide, Version 2.0. Earth Sciences Division, Lawrence Berkeley Laboratory, University of California. California 94720.

Pruess, K., O'Sullivan, M. and Kennedy, B., 2000. Modeling of Phase-Partitioning Tracers in Fractured Reservoirs. Proceedings Twenty-Fifth Workshop on Geothermal Reservoir Engineering. Stanford Geothermal Program. Stanford University, Stanford, California. Workshop Report SGP-TR-165. On CD.

Reid, R., Prausnitz, J. and Sherwood, T., 1977. The Properties of Gases and Liquids. Third edn. McGraw-Hill Book Company.

Schotte, W., 1985. Solubilities Near the Critical Point. American Institute of Chemical Engineers Journal 31(1), 154–157.

Smits, P., Peters, C. and de Swaan Arons, J., 1998. Measurement of the high-pressure-high-temperature fluid phase behaviour of the systems $CF_4 + H_2O$, $CF_4 + H_2O + NaCl$, $CHF_3 + H_2O$, and $CHF_3 + H_2O + NaCl$. Fluid Phase Equilibria 150-151, 745–751.

Trew, M., O'Sullivan, M., Harvey, C., Anderson, E. and Pruess, K., 2000. Computer Modelling of Gas and Liquid Tracers in Geothermal Reservoirs. Proceedings Twenty-Fifth Workshop on Geothermal Reservoir Engineering. Stanford Geothermal Program. Stanford University, Stanford, California. Workshop Report SGP-TR-165. On CD.

Tsai, J. and Chen, Y., 1998. Application of a volume-translated Peng-Robinson equation of state on vapor-liquid equilibrium calculations. Fluid Phase Equilibria 145, 193–215.

Twu, C., Coon, J. and Cunningham, J., 1995. A new generalized alpha function for a cubic equation of state. Part 1. Peng-Robinson equation. Fluid Phase Equilibria 105, 49–59.

Van Ness, H. and Abbott, M., 1997. Thermodynamics. In: R. Perry and D. Green (eds), Perry's Chemical Engineers' Handbook. Seventh edn. McGraw-Hill. Chapter 4.

Walas, S., 1985. Phase Equilibria in Chemical Engineering. Butterworth Publishers.

Wen, W. and Muccitelli, J., 1979. Thermodynamics of Some Perflurocarbon Gases in Water. Journal of Solution Chemistry 8(3), 225–245.

Wilhelm, E., Battino, R. and Wilcock, R., 1977. Low-Pressure Solubility of Gases in Liquid Water. Journal of Chemical Reviews 77, 219–262.

Figure Captions

Fig. 1. The definition of Henry's law as a hypothetical linear relationship of slope C_H between the liquid phase partial gas fugacity, $\hat{f}_g^l$, and the liquid mole fraction of tracer, x.

Fig. 2. Theoretically calculated infinite dilution partial molar volumes, $\hat{V}_g^l$, for a selection of gas tracers. (A) Maximum, minimum and mean $\hat{V}_g^l$ values. (B) Mean values and the empirical fit to the mean values without including molecular weight.

Fig. 3. The quality of the empirical fit to the theoretically calculated infinite dilution partial molar volumes, $\hat{V}_g^l$. The fit improves when the molecular weight is included. (A) Fitting the mean values determined from data for: SF_6, R-13, R-14, R-22, R-23, R-116, R-C318, R-134a, R-124 and R-125. (B) Using the same mean values to empirically represent the behavior of O_2 and CO_2.

Fig. 4. A comparison of Henry's law coefficients calculated using the Harvey (1996) correlation and the modified Harvey correlation. (A) SF_6. (B) R-134a. (C) R-23.

Fig. 5. Henry's law coefficient fit for SF_6. (A) At standard state. (B) The variation with temperature and pressure.

Fig. 6. Henry's law coefficient fit for R-13. (A) At standard state. (B) The variation with temperature and pressure.

Fig. 7. Henry's law coefficient fit for R-14. (A) At standard state. (B) The variation with temperature and pressure.

Fig. 8. Henry's law coefficient fit for R-22. (A) At standard state. (B) The variation with temperature and pressure.

Fig. 9. Henry's law coefficient fit for R-23. (A) At standard state. (B) The variation with temperature and pressure.

Fig. 10. Henry's law coefficient fit for R-116. (A) At standard state. (B) The variation with temperature and pressure.

Fig. 11. Henry's law coefficient fit for R-C318. (A) At standard state. (B) The variation with temperature and pressure.

Fig. 12. Henry's law coefficient fit for R-134a. (A) At standard state. (B) The variation with temperature and pressure.

Fig. 13. Henry's law coefficient fit for R-124. (A) At standard state. (B) The variation with temperature and pressure.

Fig. 14. Henry's law coefficient fit for R-125. (A) At standard state. (B) The variation with temperature and pressure.

Fig. 15. The stream-tube test problem specifications.

Fig. 16. The two-phase flow conditions at steady state in the stream-tube test problem. The distance is from the production well. (A) Pressure, P, and water vapor pressure, P_w^s, variation. (B) Temperature variation. (C) Vapor saturation variation.

Fig. 17. The tracer return curves for SF_6 in the stream-tube test problem. The time is from injection. (A) Liquid phase. (B) Vapor phase.

Fig. 18. The tracer return curves for R-134a in the stream-tube test problem. The time is from injection. (A) Liquid phase. (B) Vapor phase.

Fig. 19. The tracer return curves for R-23 in the stream-tube test problem. The time is from injection. (A) Liquid phase. (B) Vapor phase.

Fig. 20. The Temperature and vapor saturation iso-surfaces in an idealised three-dimensional reservoir. (A) $200^{\circ}\mathrm{C}$ iso-surface. (B) 10% vapor saturation iso-surface.

Fig. 21. The predicted liquid and vapor phase mass fractions of SF_6 in an idealised three-dimensional reservoir over 100 days. (A) Following injection. (B) After 50 days. (C) After 100 days.

Table Captions

Table 1
The molecular weight (M), critical temperature (T^c), critical pressure (P^c), acentric factor (ω), and modified Harvey correlation coefficients (A^*, B^* and C^*) for water and a selection of gas tracers.

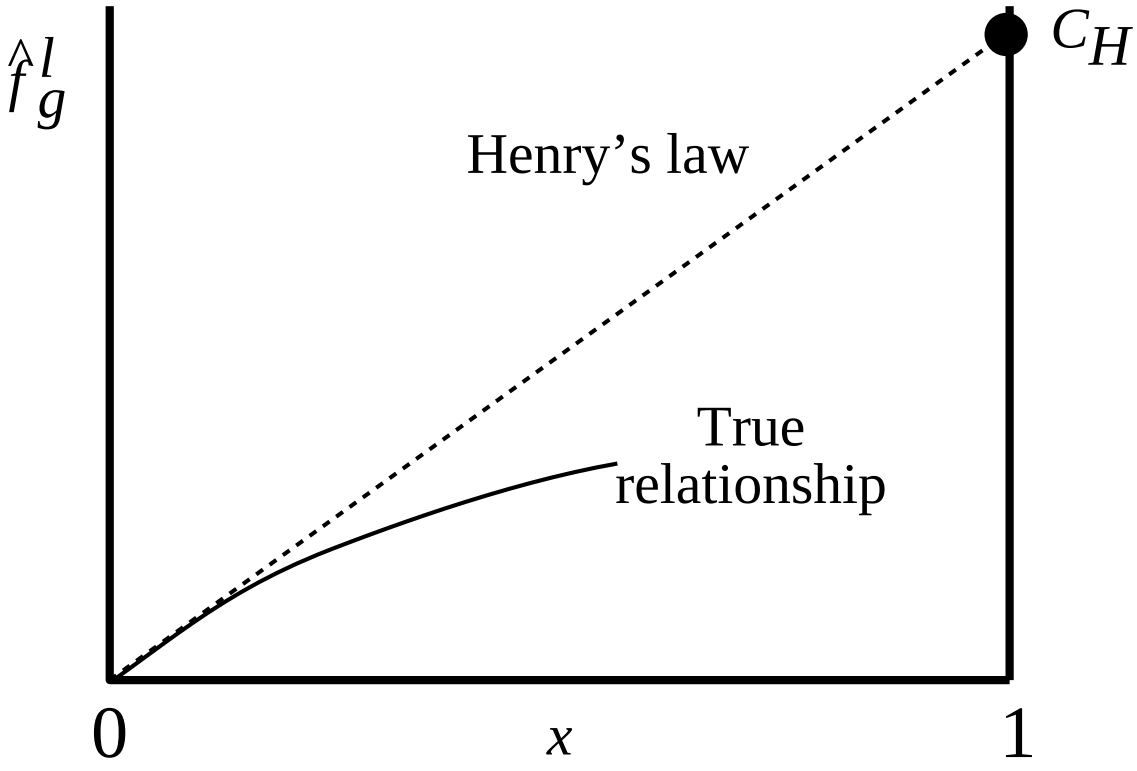
$\hat{f}_g^l$
C_H
Henry's law
True
relationship
0
x
1

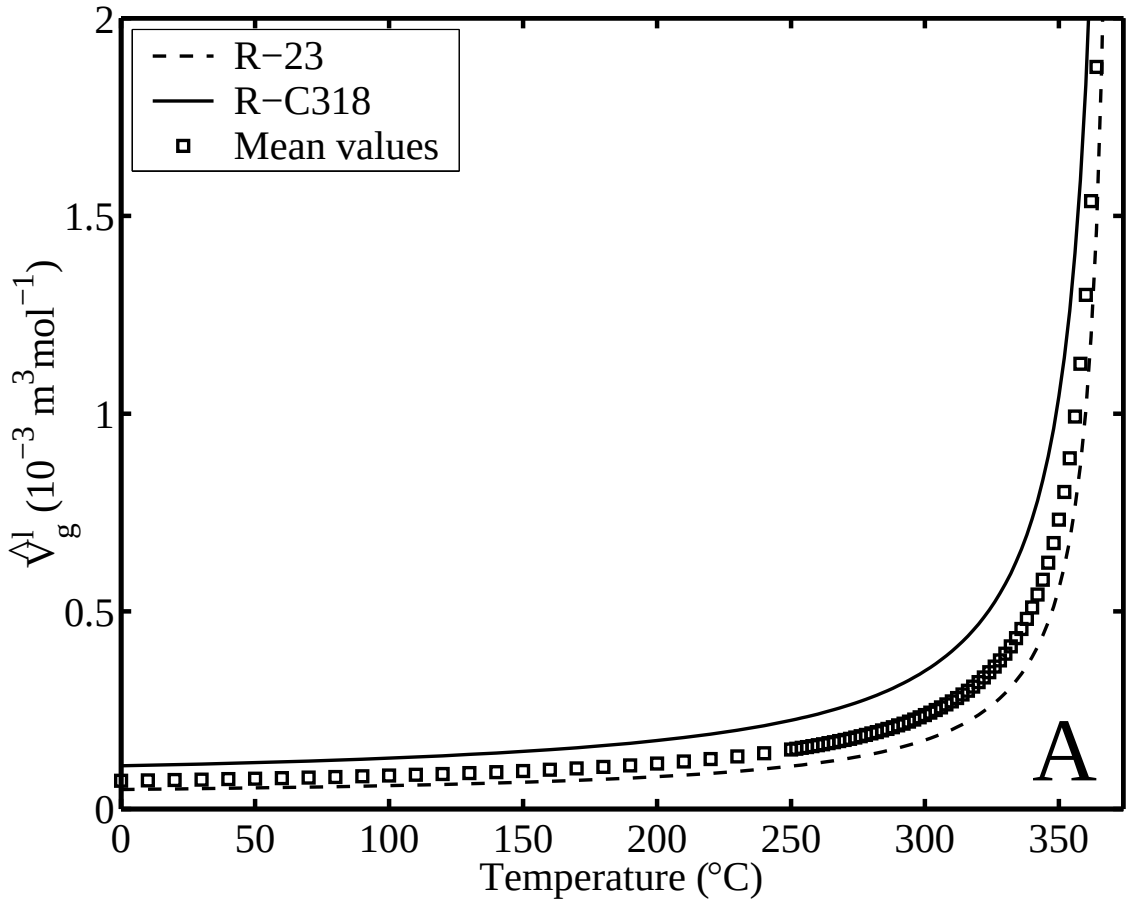
R−23
R−C318
Mean values
A
$\Delta_g^l V$ (10^{-3} $m^3 mol^{-1}$)
Temperature (°C)
0
0.5
1
1.5
2
0
50
100
150
200
250
300
350

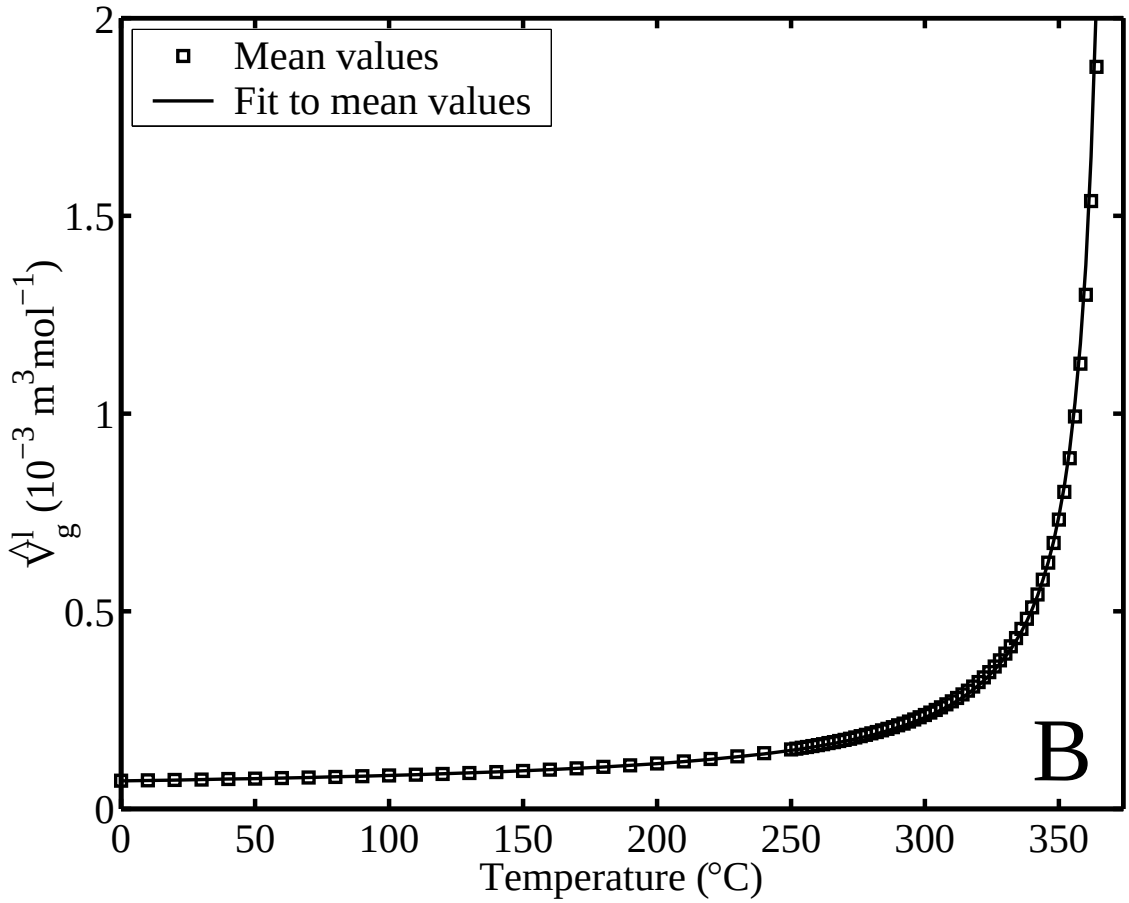
Mean values
Fit to mean values
B
$\Delta_g^l V$ (10^{-3} $m^3 mol^{-1}$)
Temperature (°C)
0
0.5
1
1.5
2
0
50
100
150
200
250
300
350

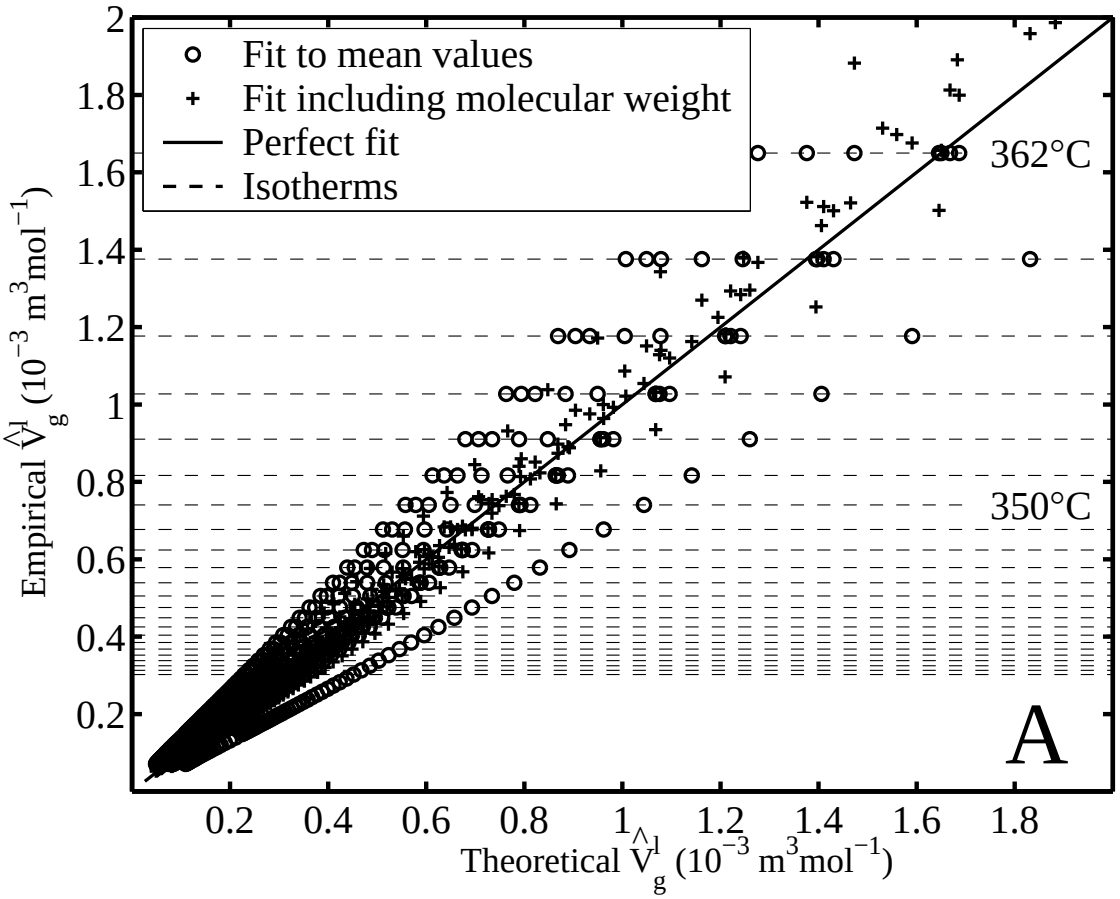
Fit to mean values
Fit including molecular weight
Perfect fit
Isotherms
362°C
350°C
A
Empirical $\hat{V}_g^l$ (10^{-3} m^3mol^{-1})
Theoretical $\hat{V}_g^l$ (10^{-3} m^3mol^{-1})
0.2
0.4
0.6
0.8
1
1.2
1.4
1.6
1.8
2

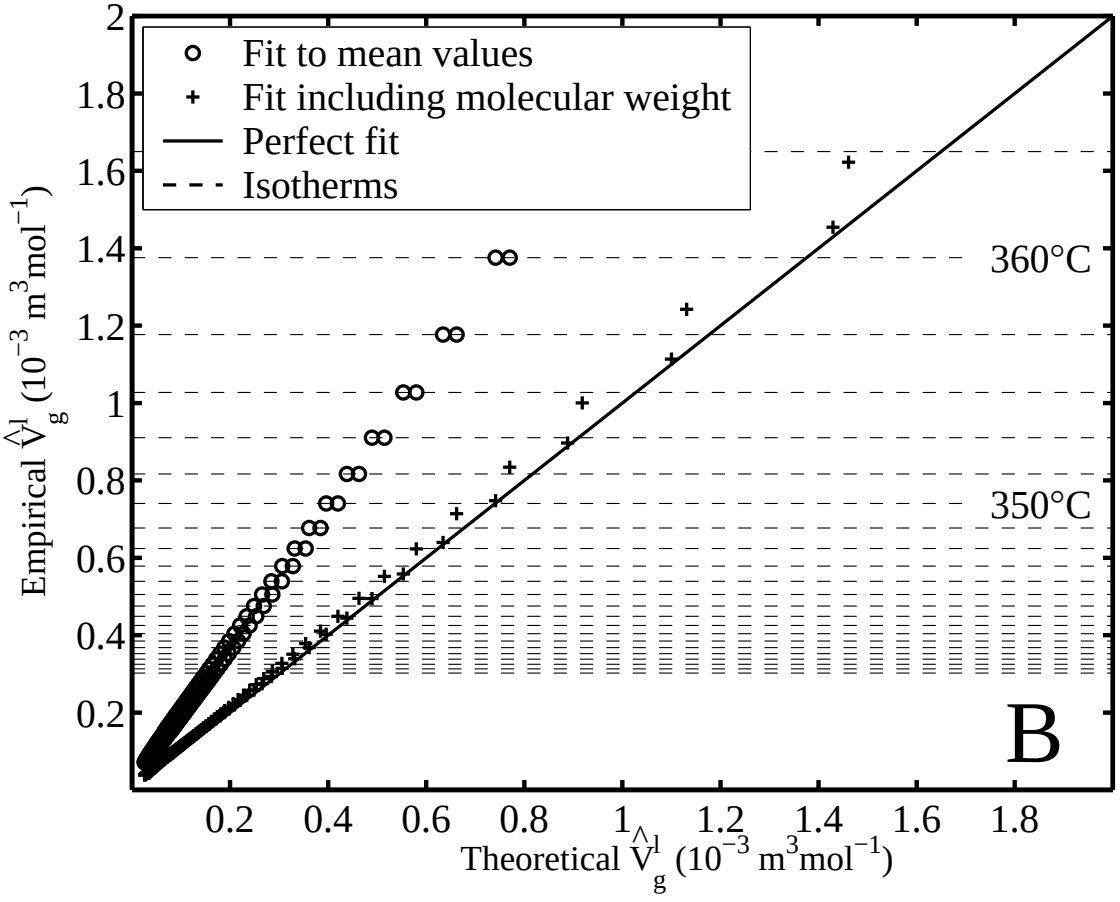
Fit to mean values
Fit including molecular weight
Perfect fit
Isotherms
360°C
350°C
B
Empirical $\hat{V}_g^l$ (10^{-3} m^3mol^{-1})
Theoretical $\hat{V}_g^l$ (10^{-3} m^3mol^{-1})
0.2
0.4
0.6
0.8
1
1.2
1.4
1.6
1.8
2

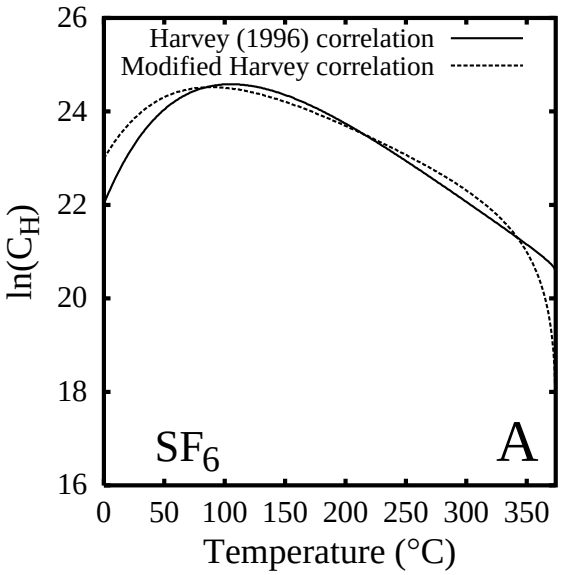
Harvey (1996) correlation
Modified Harvey correlation
ln(C_H)
26
24
22
20
18
16
0 50 100 150 200 250 300 350
Temperature (°C)
SF6
A

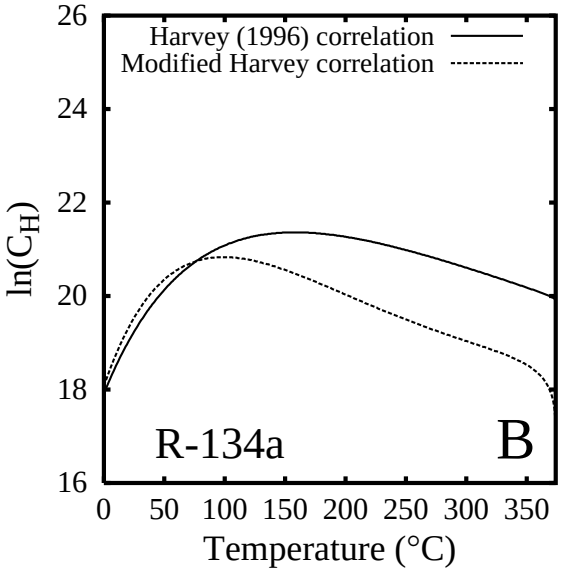
Harvey (1996) correlation
Modified Harvey correlation
ln(C_H)
26
24
22
20
18
16
0 50 100 150 200 250 300 350
Temperature (°C)
R-134a
B

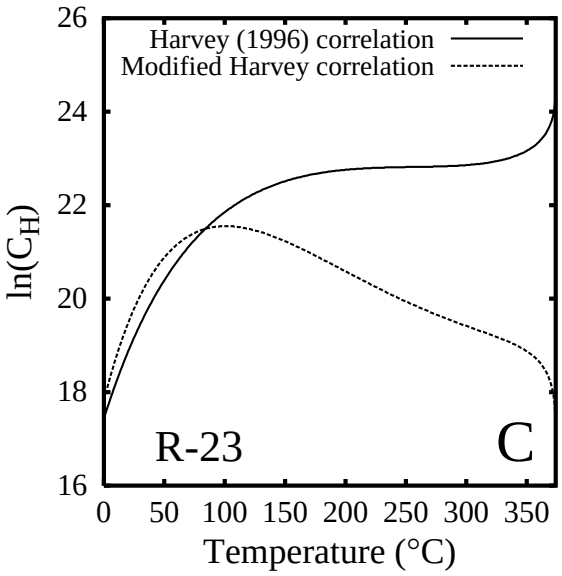
Harvey (1996) correlation
Modified Harvey correlation
ln(C_H)
26
24
22
20
18
16
0 50 100 150 200 250 300 350
Temperature (°C)
R-23
C

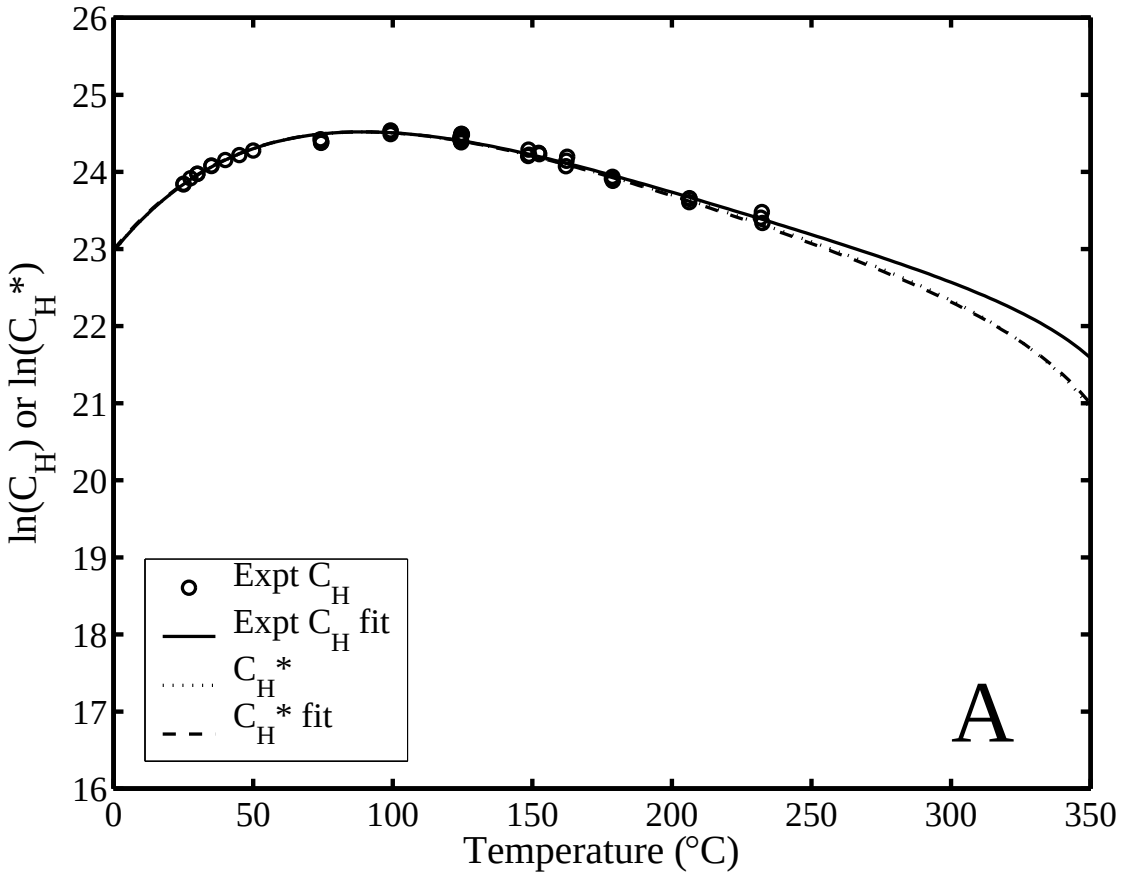
26
25
24
23
22
21
20
19
18
17
16
0
50
100
150
200
250
300
350
Temperature (°C)
ln(C_H) or ln(C_H*)
Expt C_H
Expt C_H fit
C_H*
C_H* fit
A

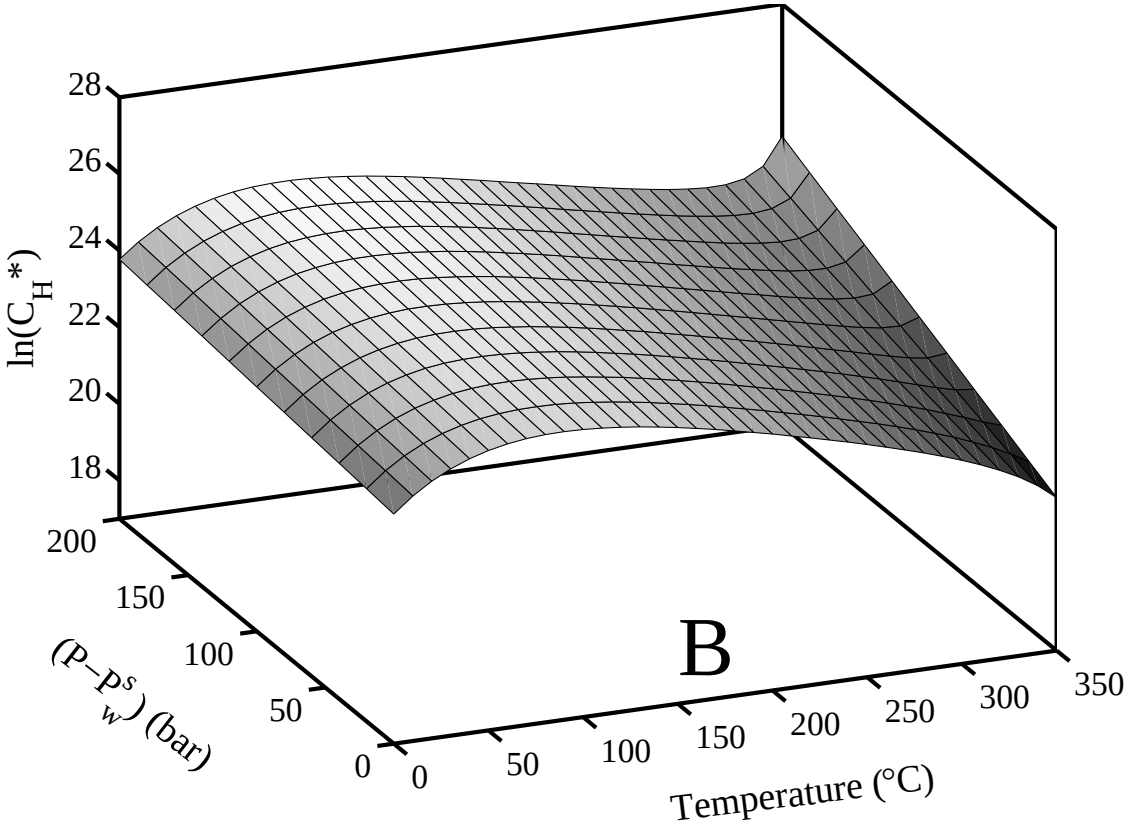
28
26
24
22
20
18
ln(C_H*)
200
150
100
50
0
(P–P^s_w) (bar)
0
50
100
150
200
250
300
350
Temperature (°C)
B

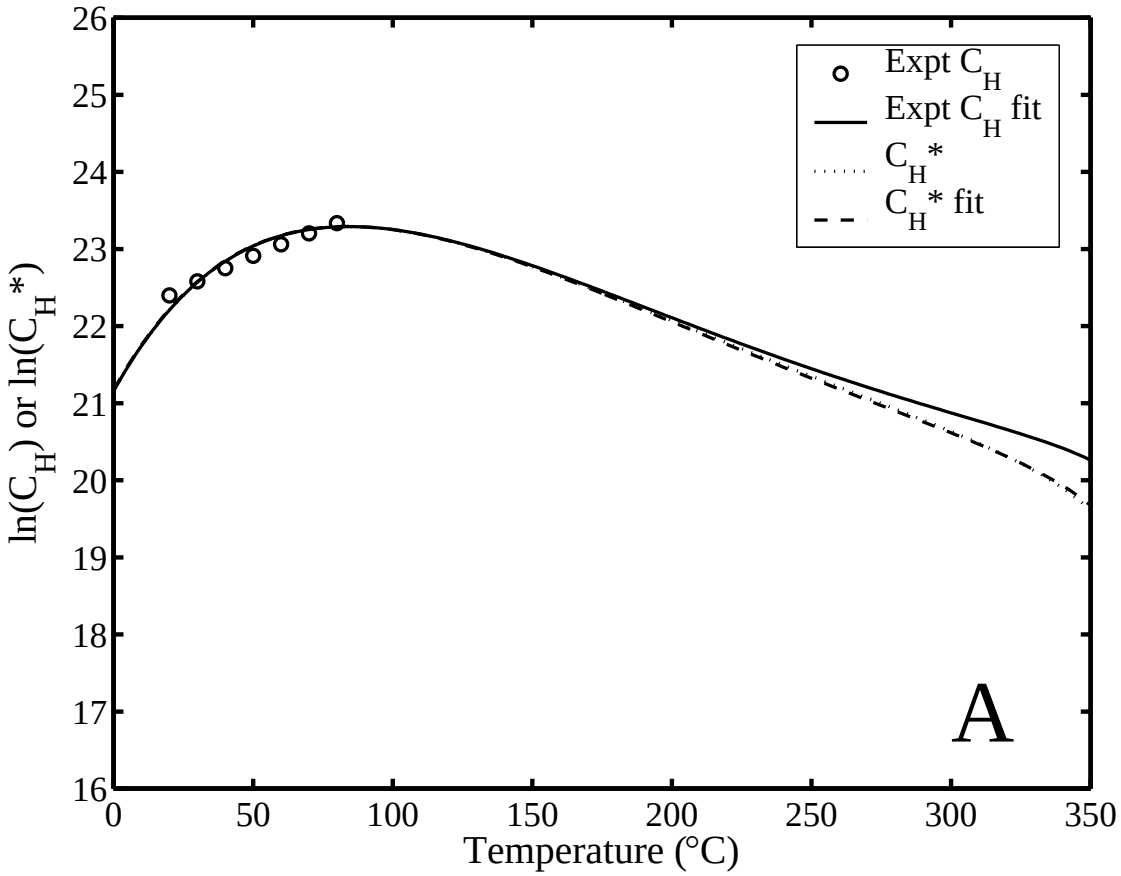
Expt C_H
Expt C_H fit
C_H*
C_H* fit
$\ln(C_H)$ or $\ln(C_H^*)$
Temperature (°C)
A

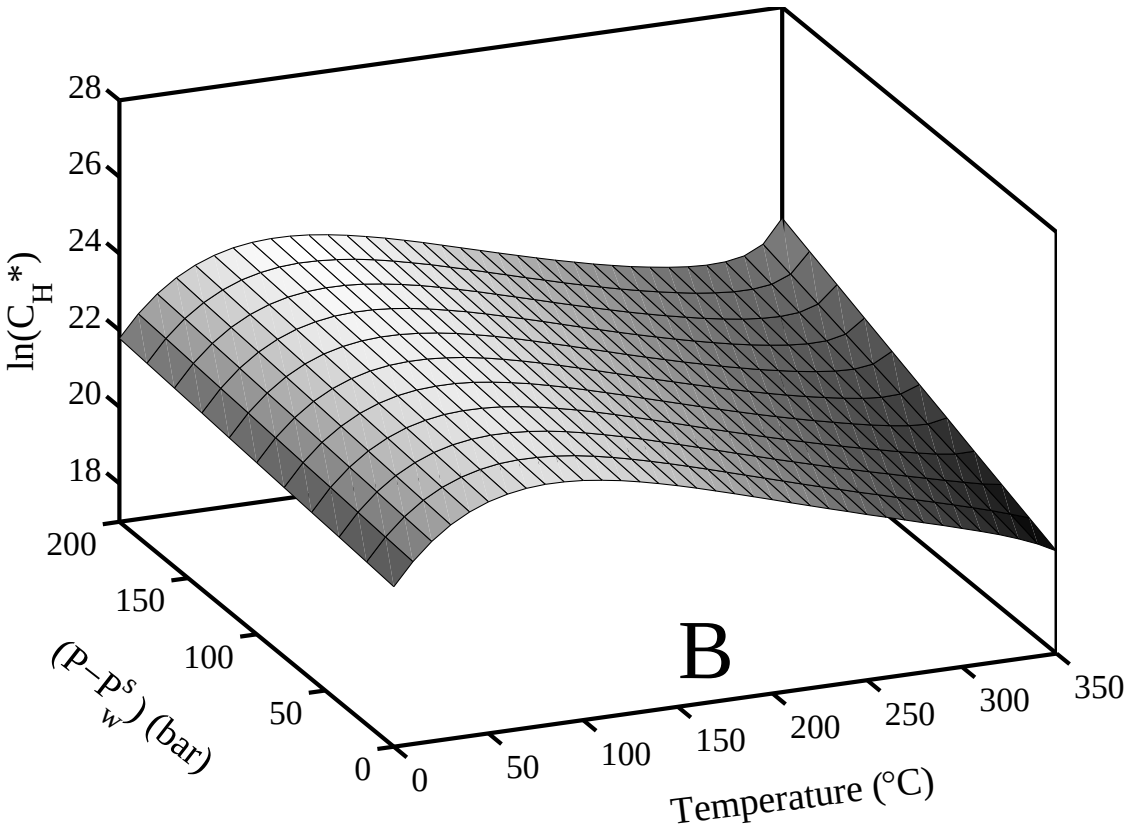
$\ln(C_H^*)$
$(P-P^s_w)$ (bar)
Temperature (°C)
B

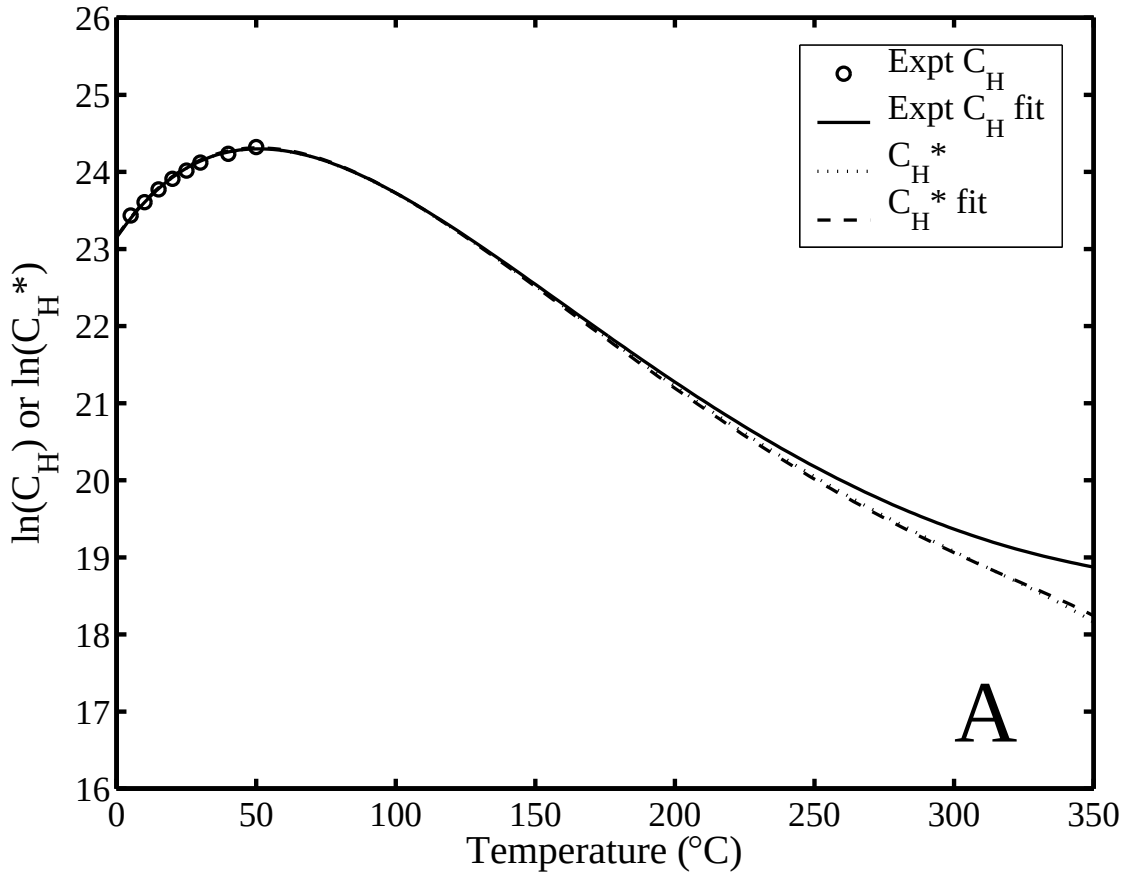
Expt C_H
Expt C_H fit
C_H*
C_H* fit
$\ln(C_H)$ or $\ln(C_H^*)$
Temperature (°C)
A

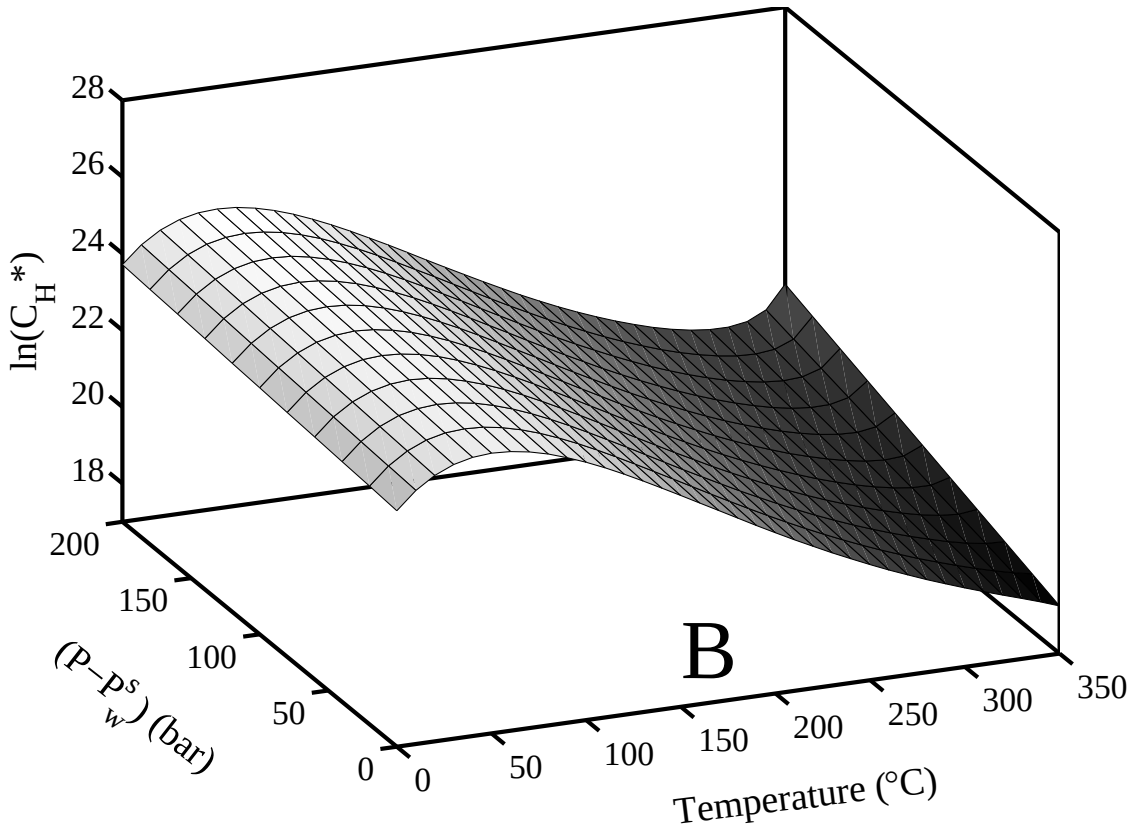
$\ln(C_H^*)$
$(P-P^s_w)$ (bar)
Temperature (°C)
B

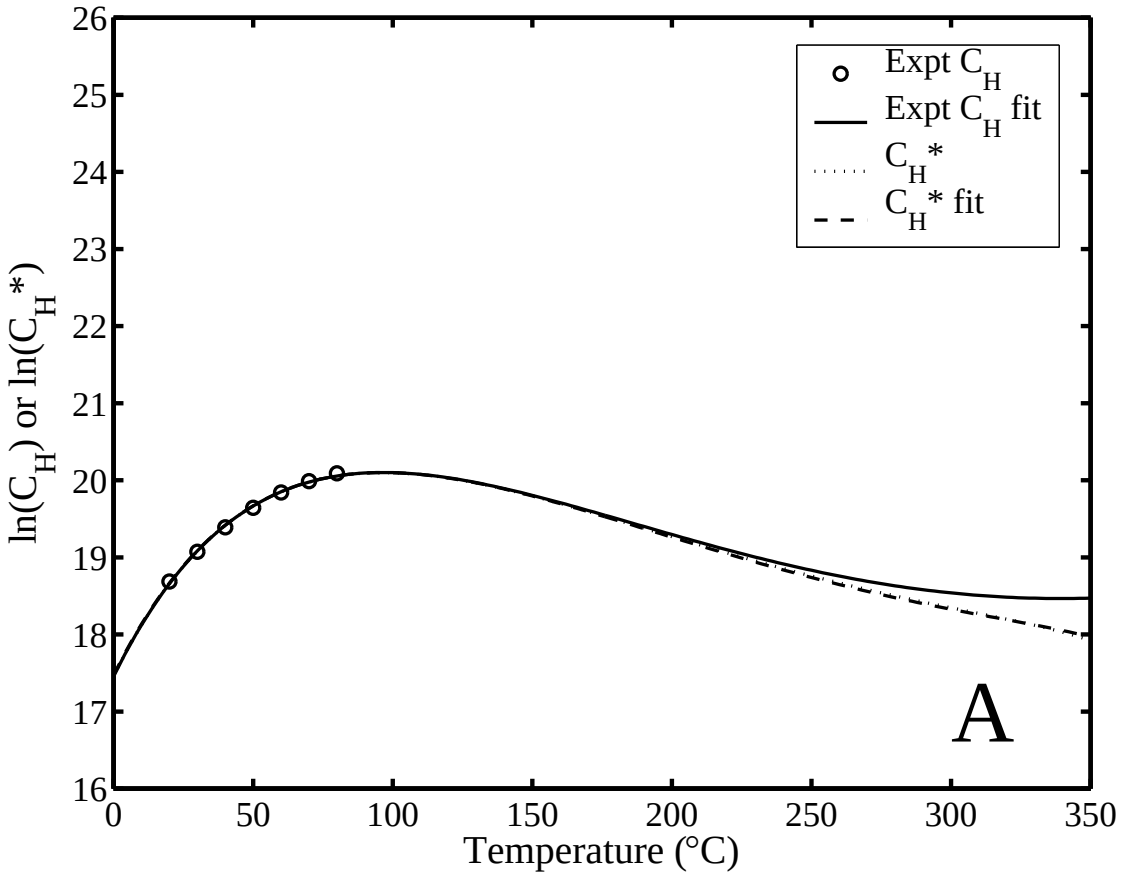
Expt C_H
Expt C_H fit
C_H*
C_H* fit
$\ln(C_H)$ or $\ln(C_H^*)$
Temperature (°C)
A

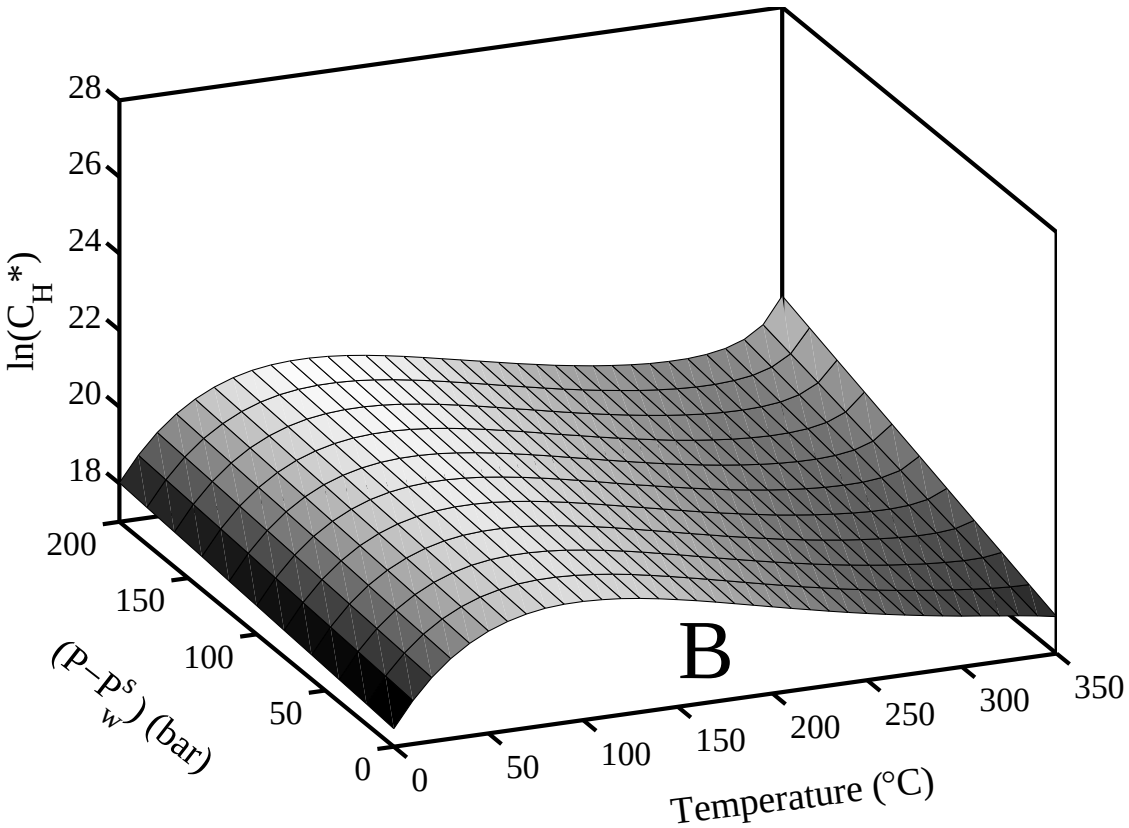
$\ln(C_H^*)$
$(P-P^s_w)$ (bar)
Temperature (°C)
B

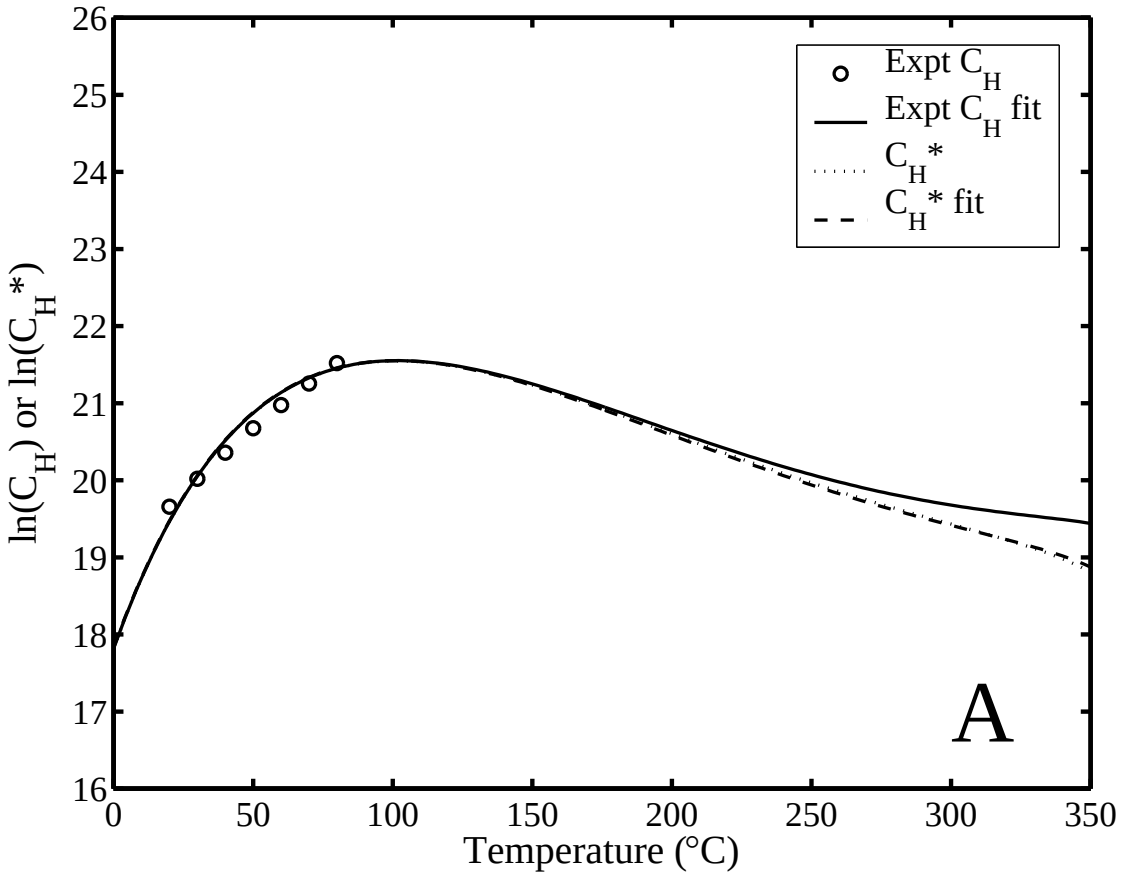
Expt C_H
Expt C_H fit
C_H*
C_H* fit
$\ln(C_H)$ or $\ln(C_H^*)$
Temperature (°C)
A

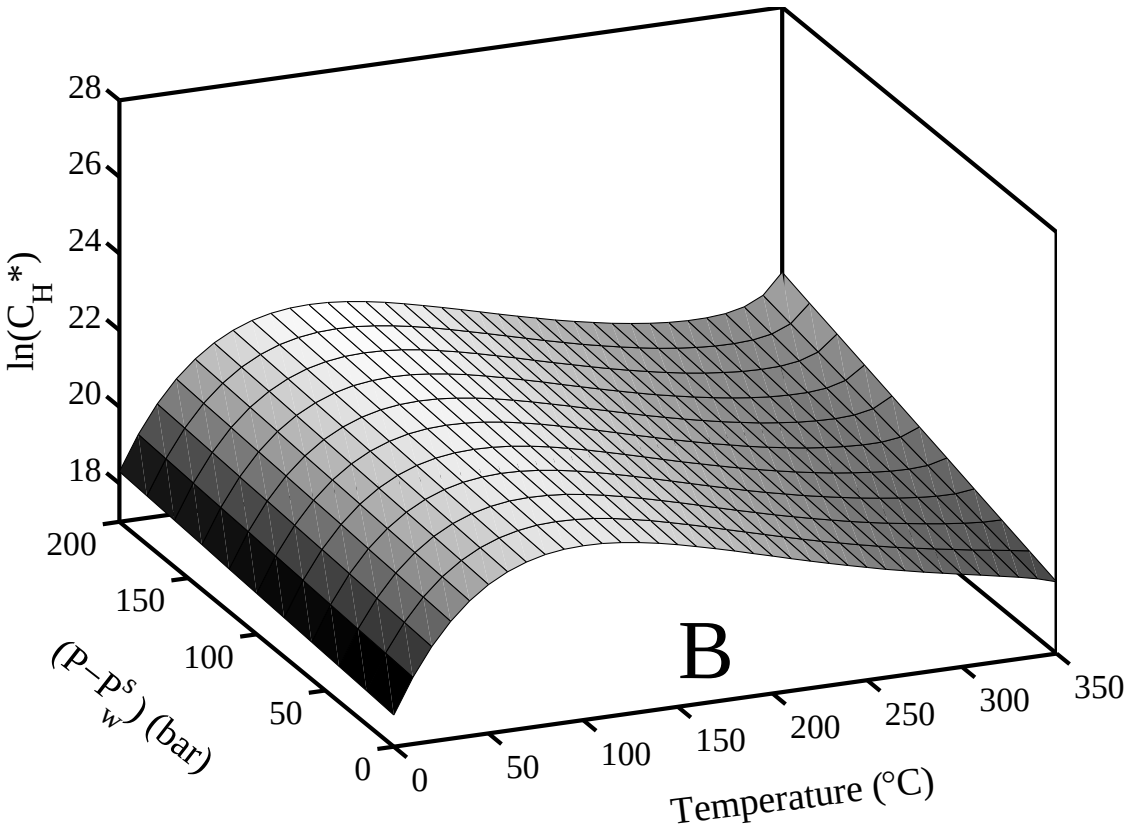
$\ln(C_H^*)$
$(P-P^s_w)$ (bar)
Temperature (°C)
B

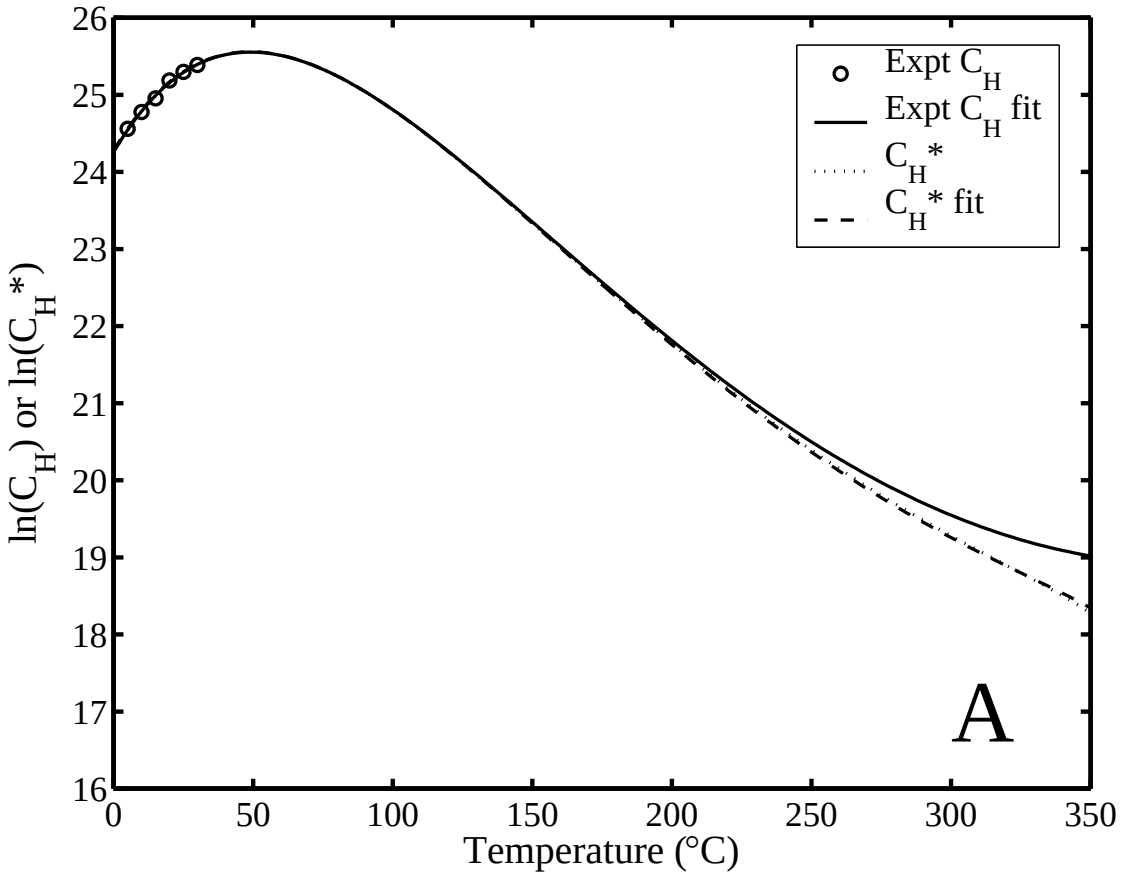
Expt C_H
Expt C_H fit
C_H*
C_H* fit
$\ln(C_H)$ or $\ln(C_H^*)$
Temperature (°C)
A

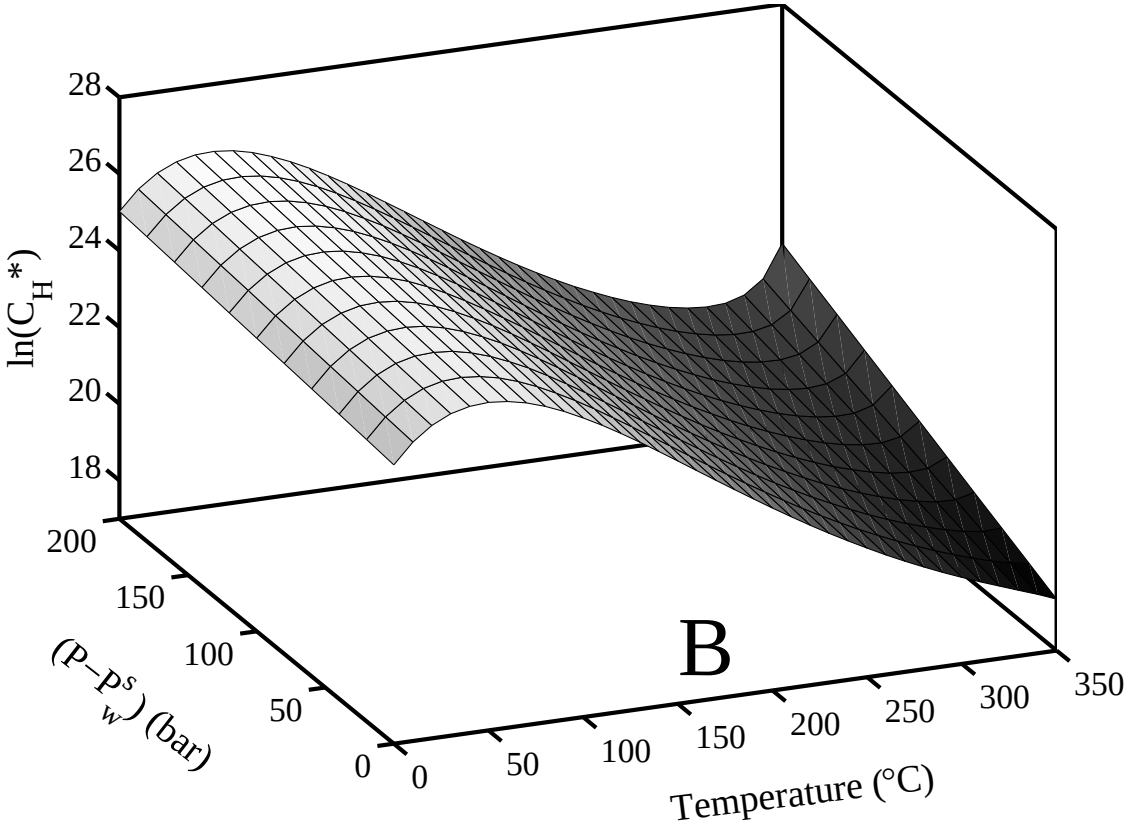
$\ln(C_H^*)$
$(P-P^s_w)$ (bar)
Temperature (°C)
B

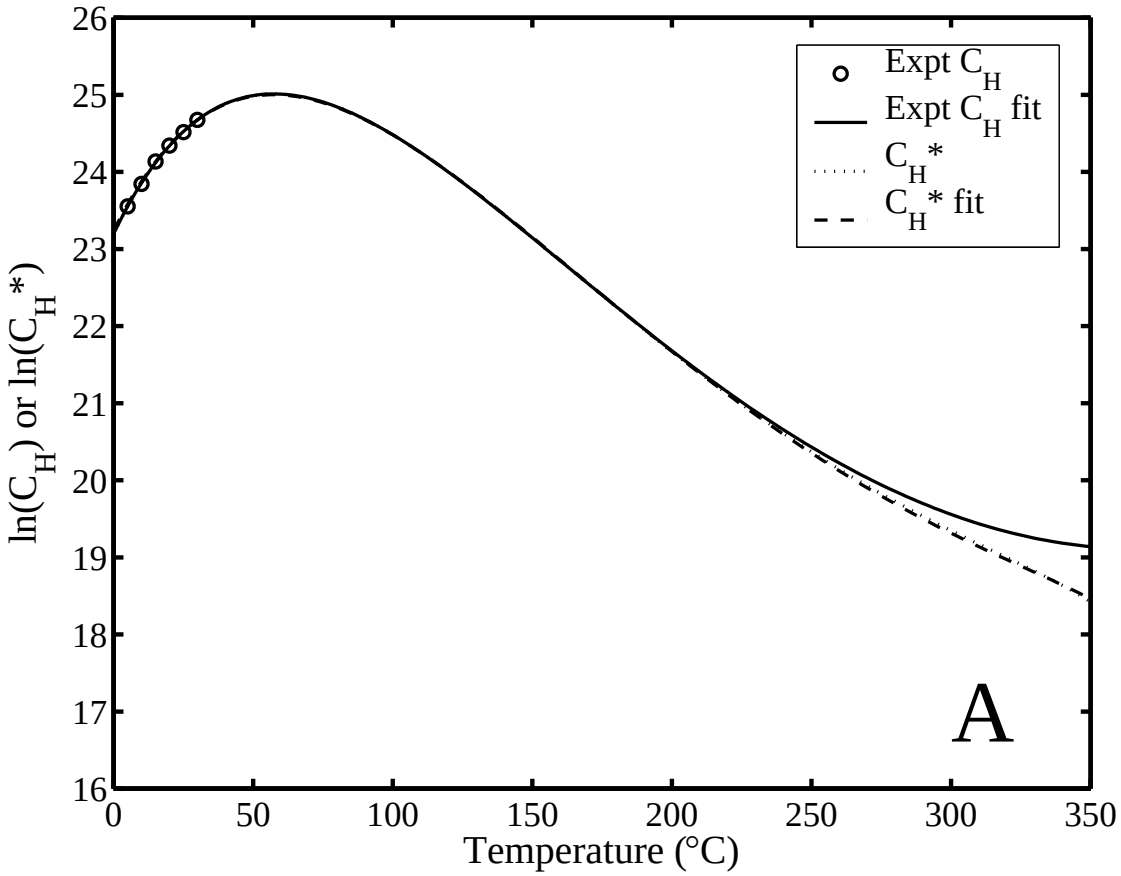
Expt C_H
Expt C_H fit
C_H*
C_H* fit
$\ln(C_H)$ or $\ln(C_H^*)$
Temperature (°C)
A

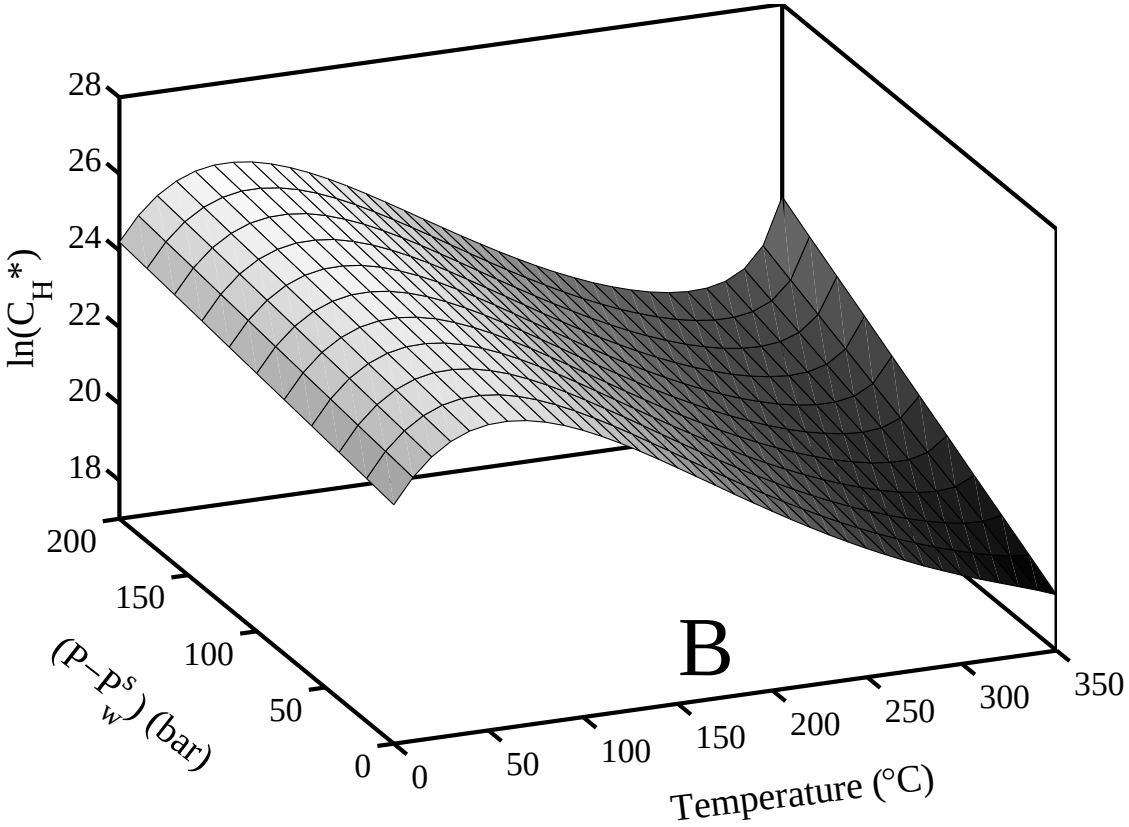
$\ln(C_H^*)$
$(P-P^s_w)$ (bar)
Temperature (°C)
B

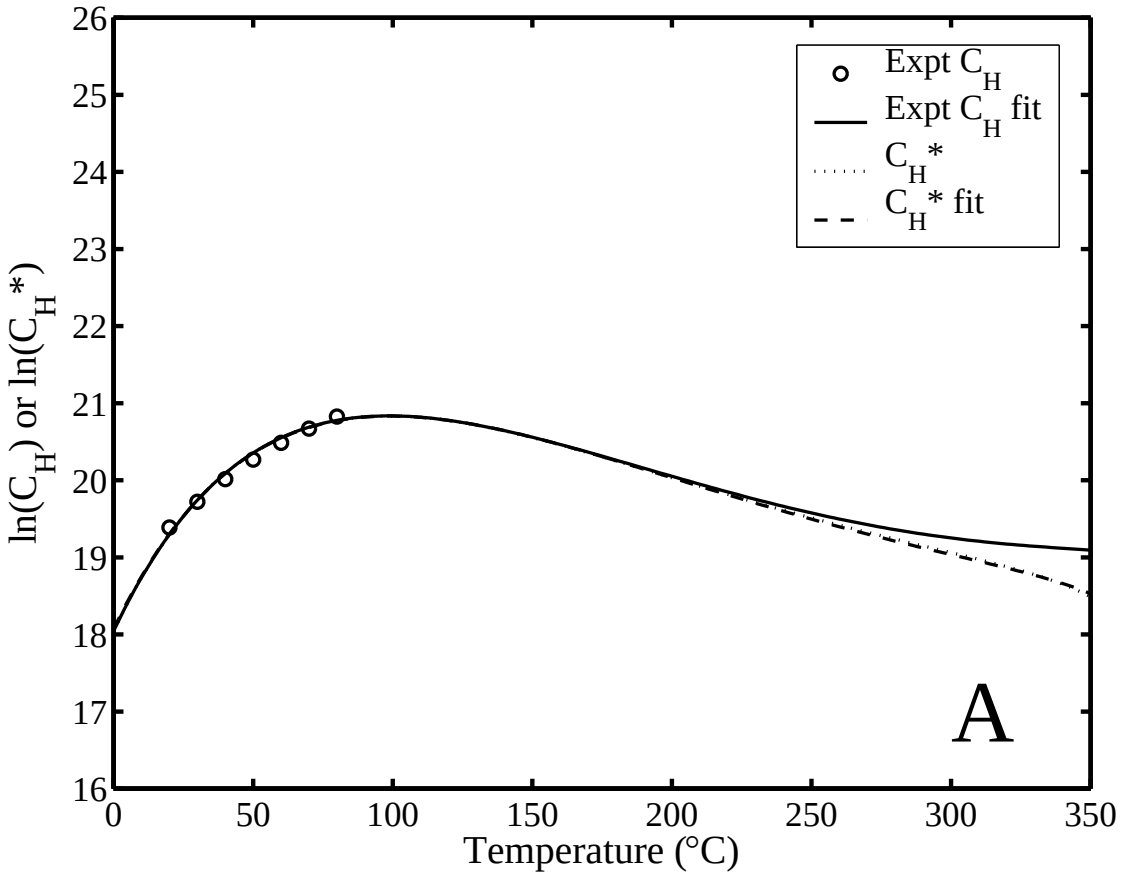
Expt C_H
Expt C_H fit
C_H*
C_H* fit
$\ln(C_H)$ or $\ln(C_H^*)$
Temperature (°C)
A

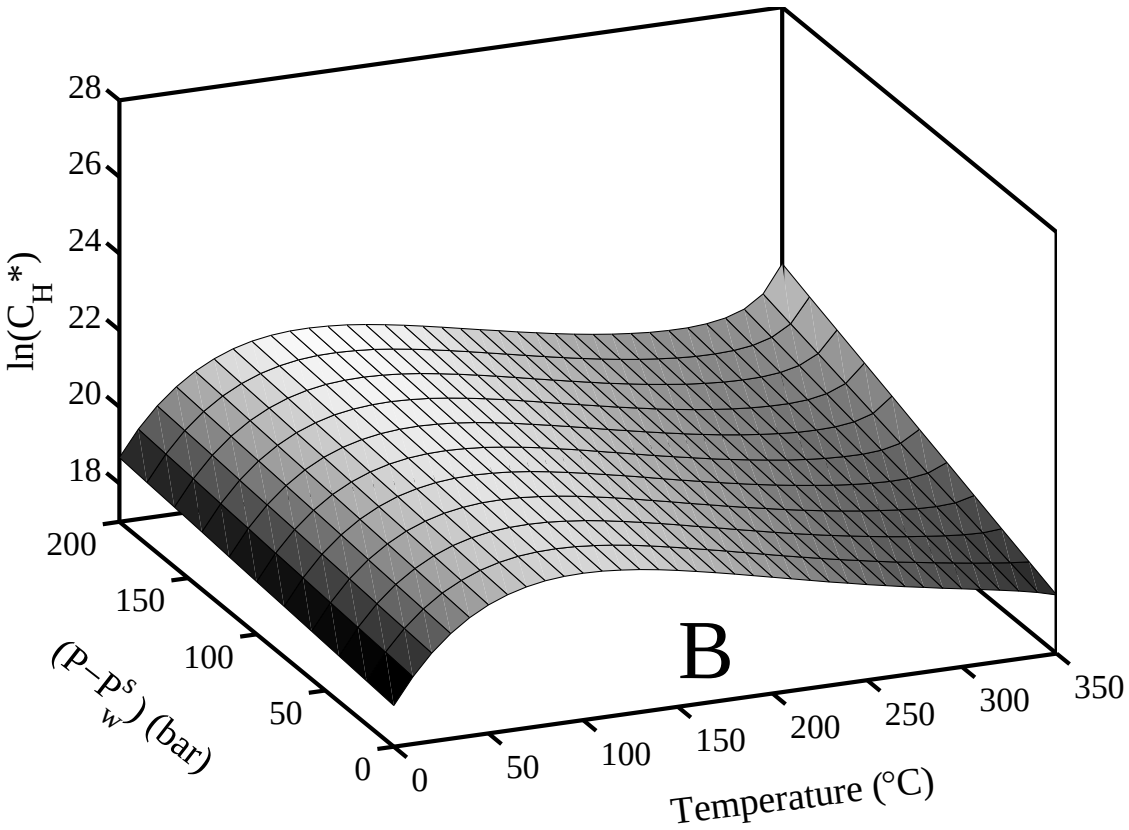
$\ln(C_H^*)$
$(P-P^s_w)$ (bar)
Temperature (°C)
B

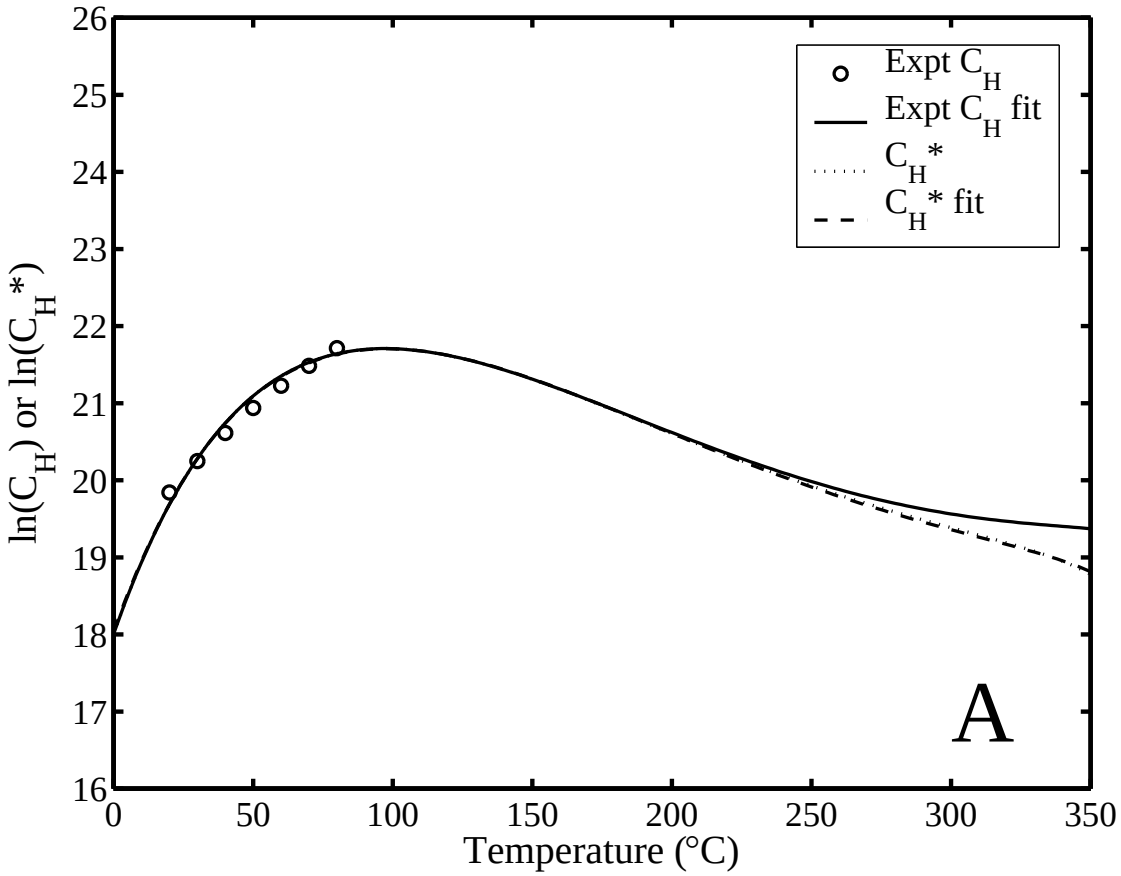
Expt C_H
Expt C_H fit
C_H*
C_H* fit
$\ln(C_H)$ or $\ln(C_H^*)$
Temperature (°C)
A

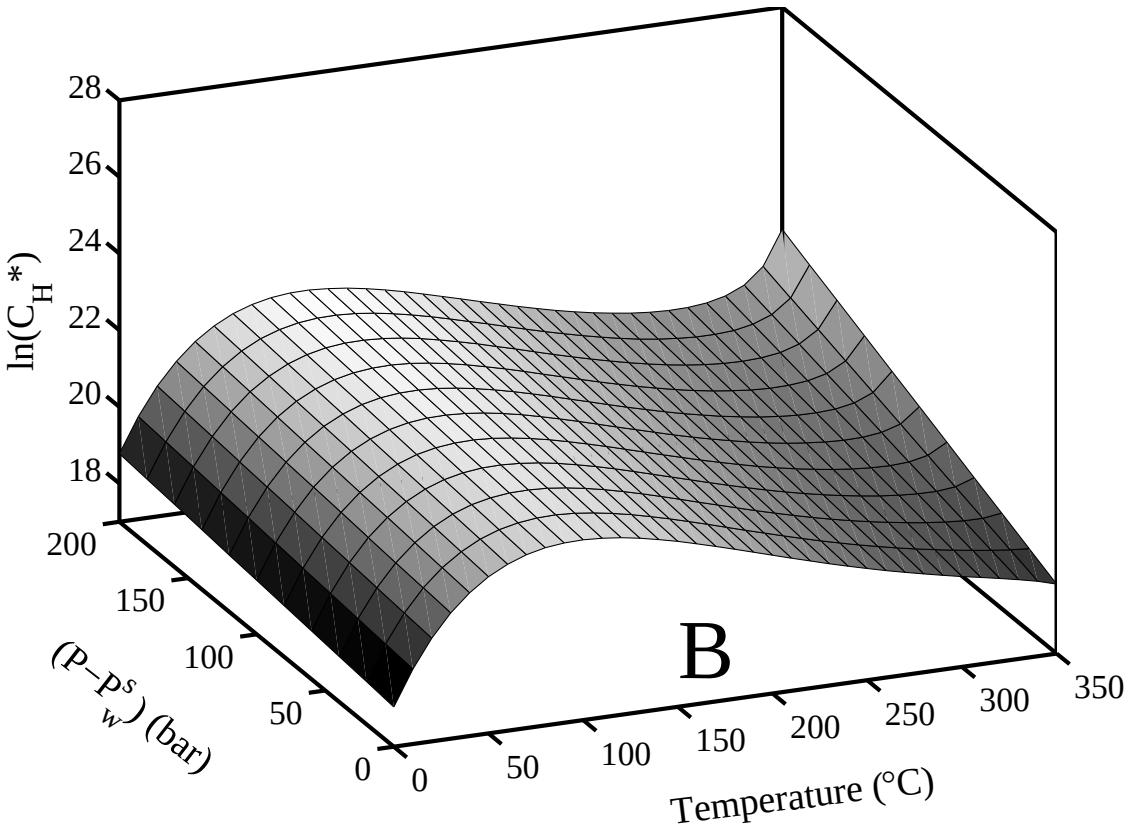
$\ln(C_H^*)$
$(P-P^s_w)$ (bar)
Temperature (°C)
B

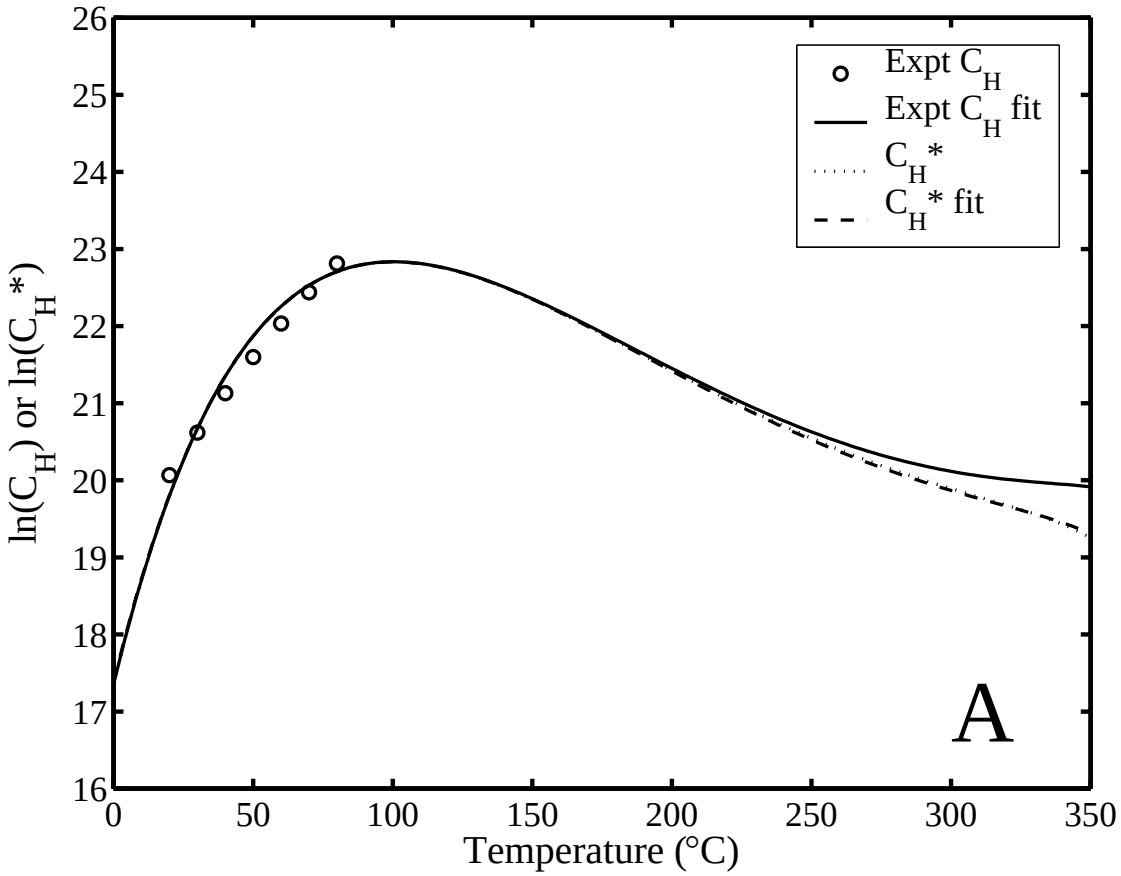
Expt C_H
Expt C_H fit
C_H*
C_H* fit
$\ln(C_H)$ or $\ln(C_H^*)$
Temperature (°C)
A

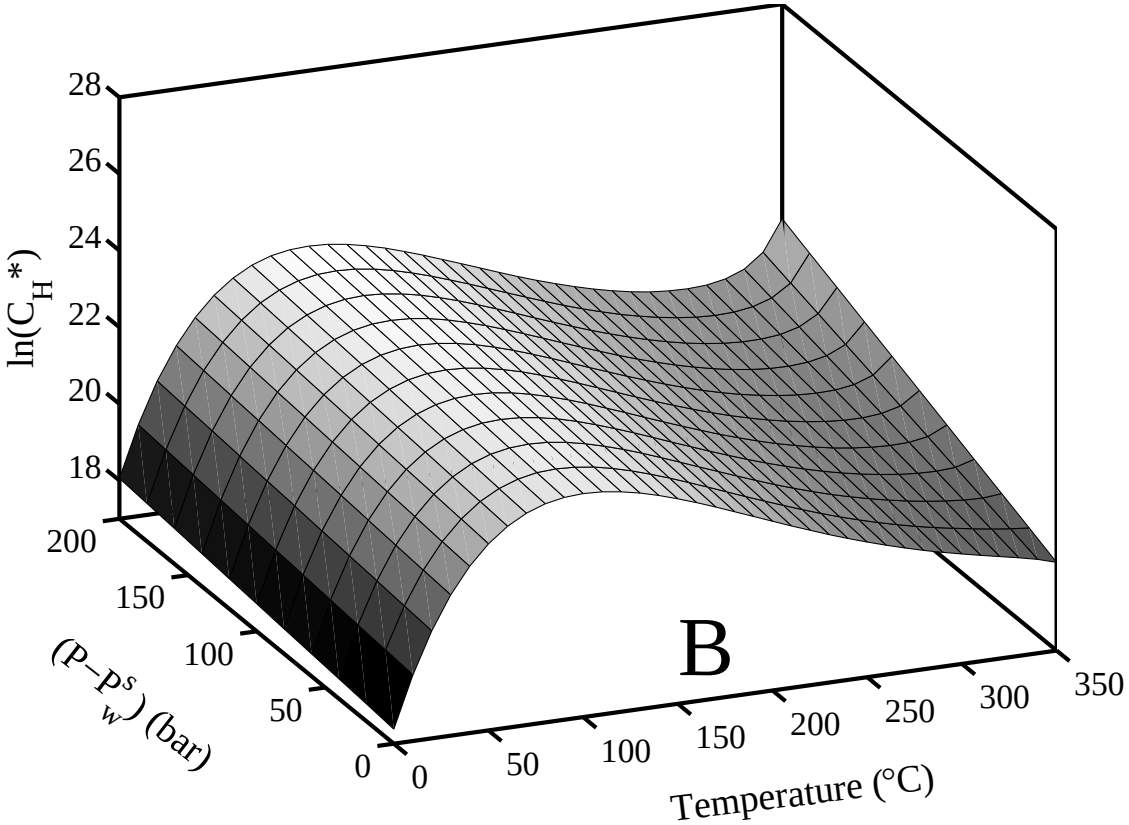
$\ln(C_H^*)$
$(P-P^s_w)$ (bar)
Temperature (°C)
B

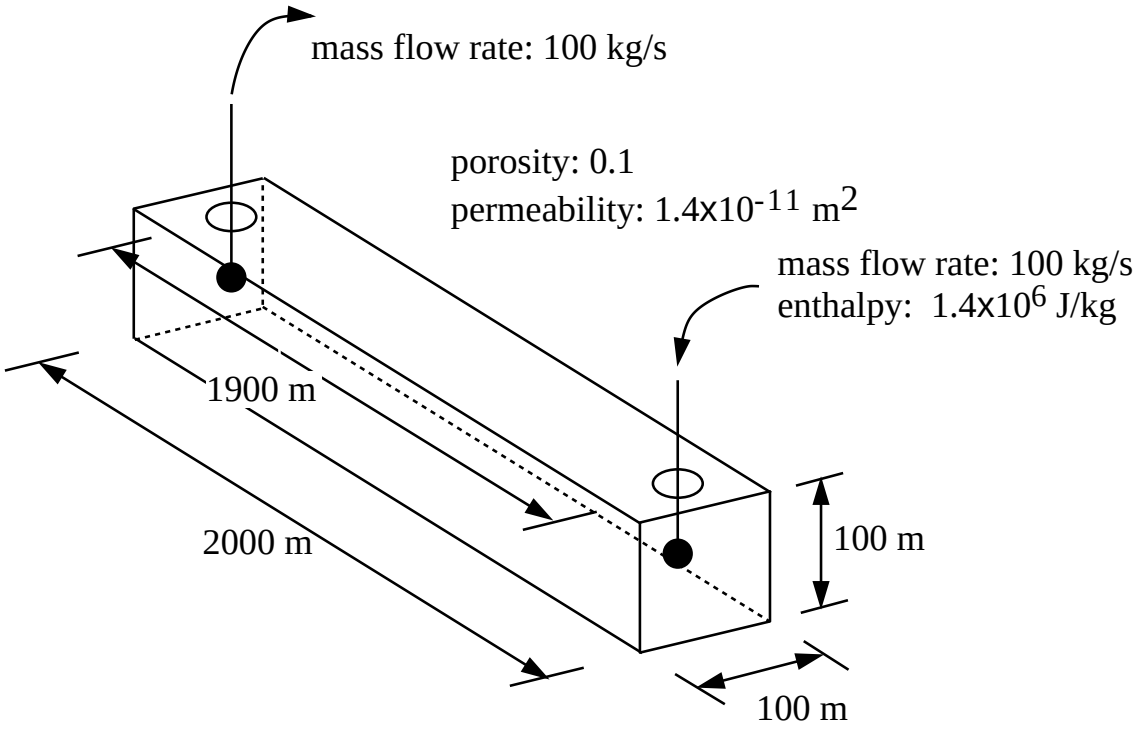
mass flow rate: 100 kg/s
porosity: 0.1
permeability: 1.4x10-11 m2
mass flow rate: 100 kg/s
enthalpy: 1.4x106 J/kg
1900 m
2000 m
100 m
100 m

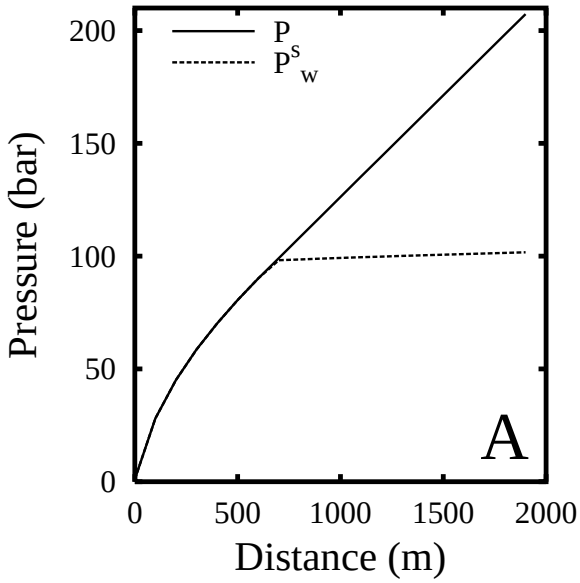
P
P^s_w
Pressure (bar)
200
150
100
50
0
0
500
1000
1500
2000
Distance (m)
A

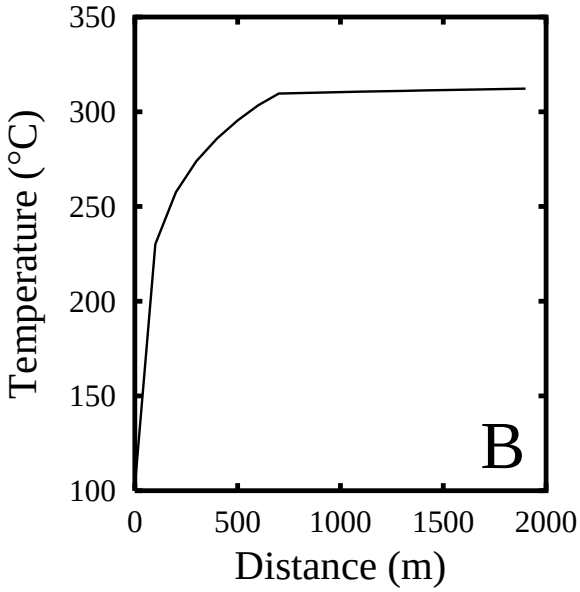
Temperature (°C)
350
300
250
200
150
100
0
500
1000
1500
2000
Distance (m)
B

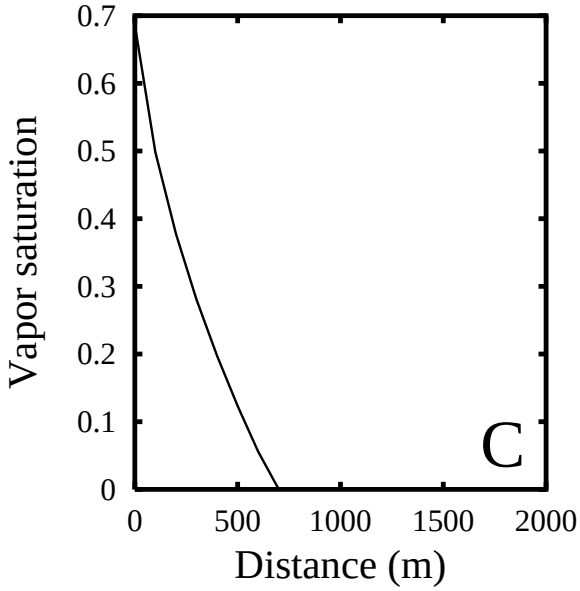
Vapor saturation
0.7
0.6
0.5
0.4
0.3
0.2
0.1
0
0
500
1000
1500
2000
Distance (m)
C

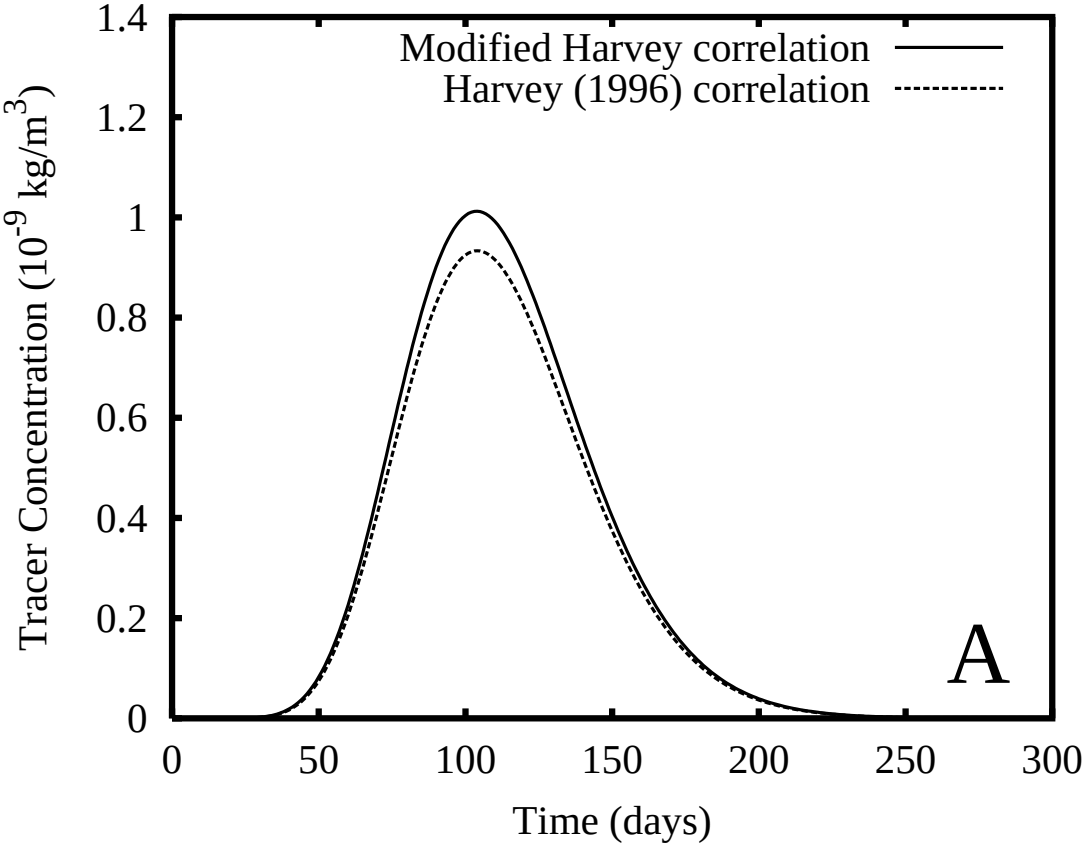
Modified Harvey correlation
Harvey (1996) correlation
Tracer Concentration (10^{-9} kg/m^3)
Time (days)
A
0
0.2
0.4
0.6
0.8
1
1.2
1.4
0
50
100
150
200
250
300

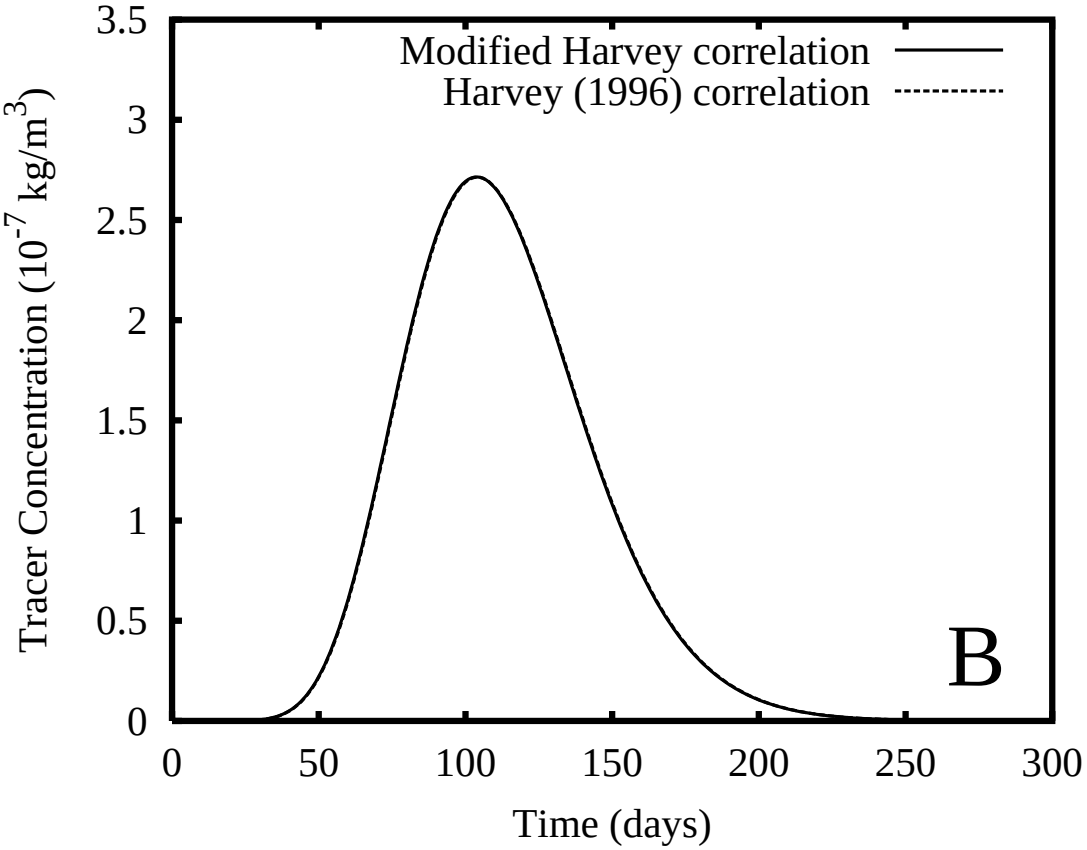
Modified Harvey correlation
Harvey (1996) correlation
Tracer Concentration (10^{-7} kg/m^3)
Time (days)
B
0
0.5
1
1.5
2
2.5
3
3.5
0
50
100
150
200
250
300

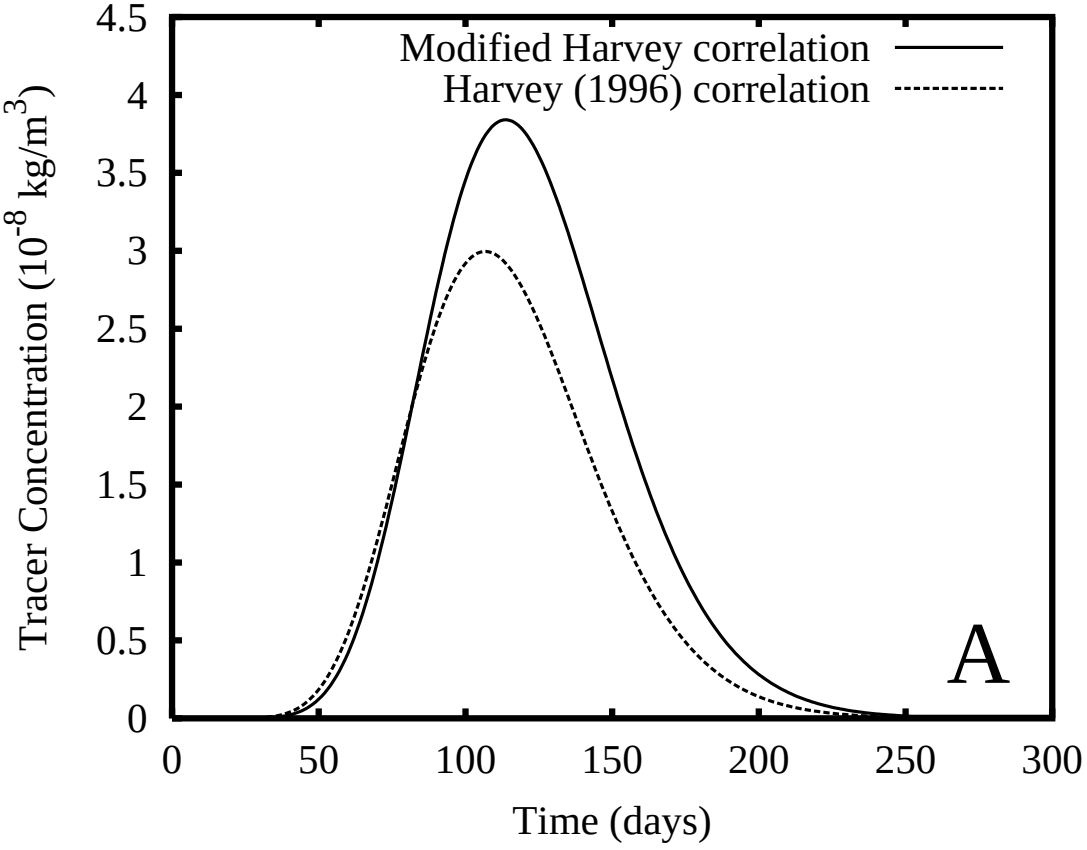
Modified Harvey correlation
Harvey (1996) correlation
Tracer Concentration (10^{-8} kg/m^3)
Time (days)
A
0
0.5
1
1.5
2
2.5
3
3.5
4
4.5
0
50
100
150
200
250
300

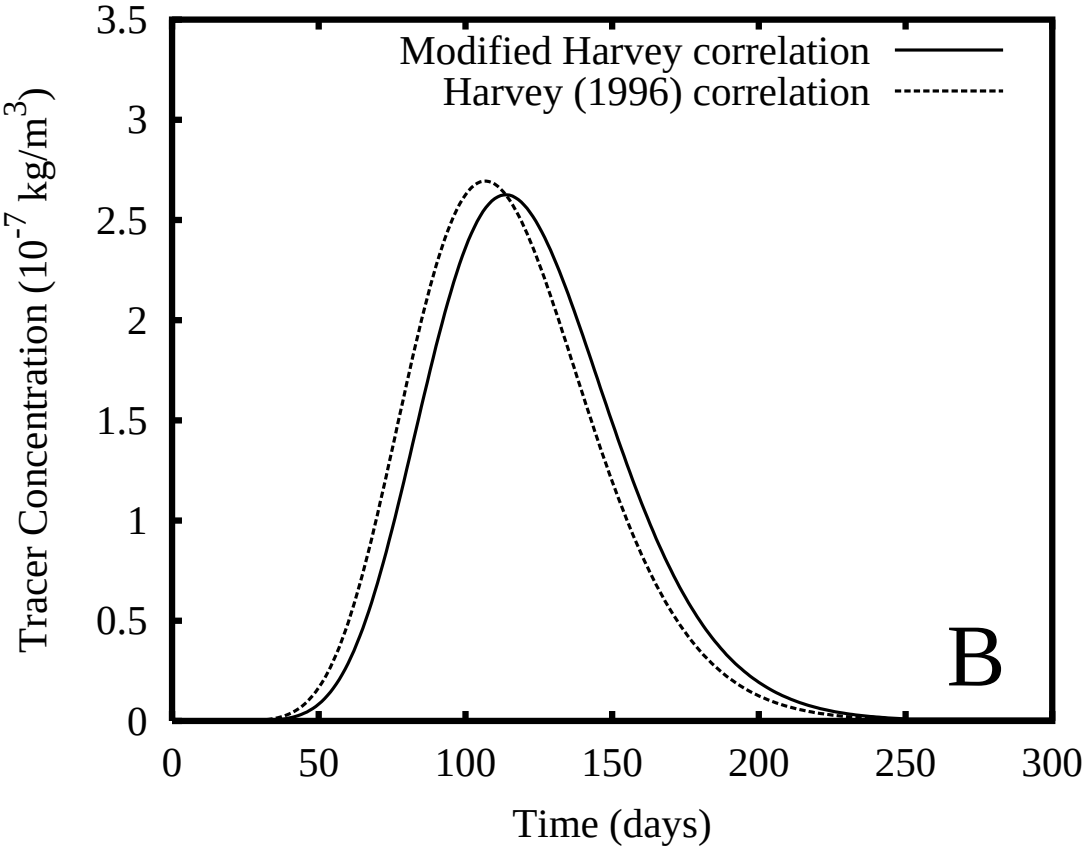
Modified Harvey correlation
Harvey (1996) correlation
Tracer Concentration (10^{-7} kg/m^3)
Time (days)
B
0
0.5
1
1.5
2
2.5
3
3.5
0
50
100
150
200
250
300

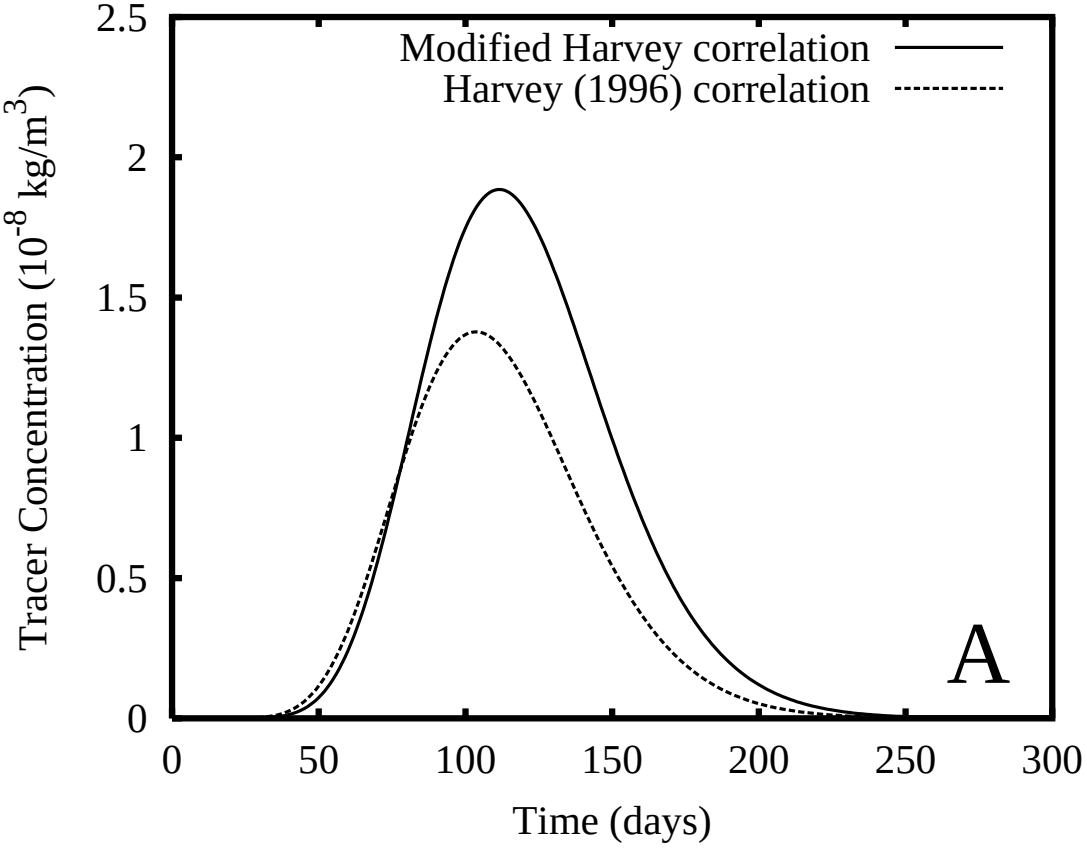
Modified Harvey correlation
Harvey (1996) correlation
Tracer Concentration (10^{-8} kg/m^3)
Time (days)
A
0
0.5
1
1.5
2
2.5
0
50
100
150
200
250
300

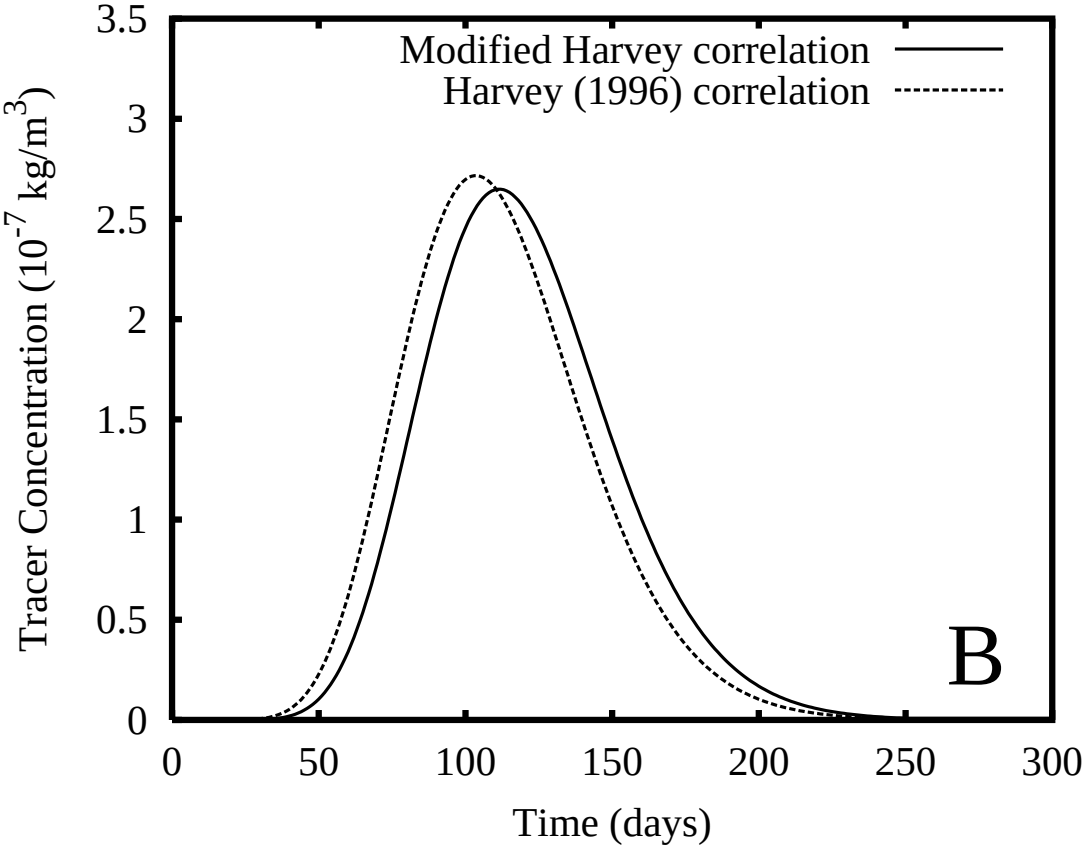
Modified Harvey correlation
Harvey (1996) correlation
Tracer Concentration (10^{-7} kg/m^3)
Time (days)
B
0
0.5
1
1.5
2
2.5
3
3.5
0
50
100
150
200
250
300

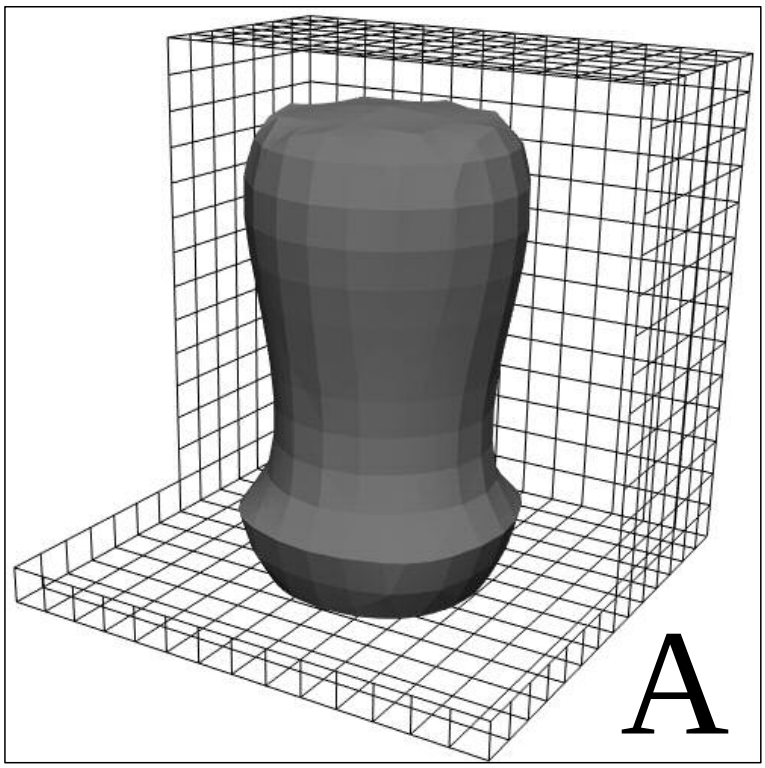
A

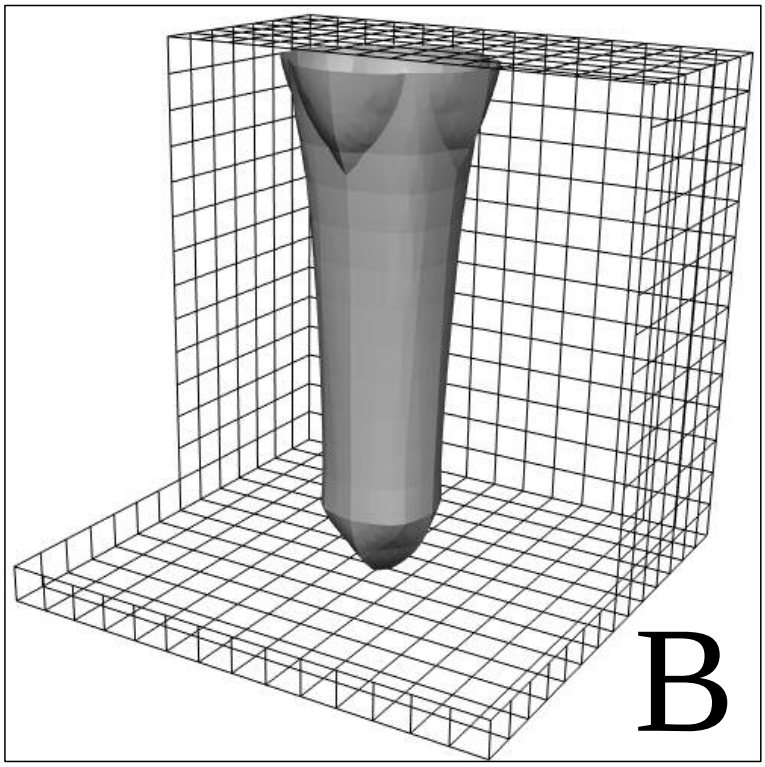
B

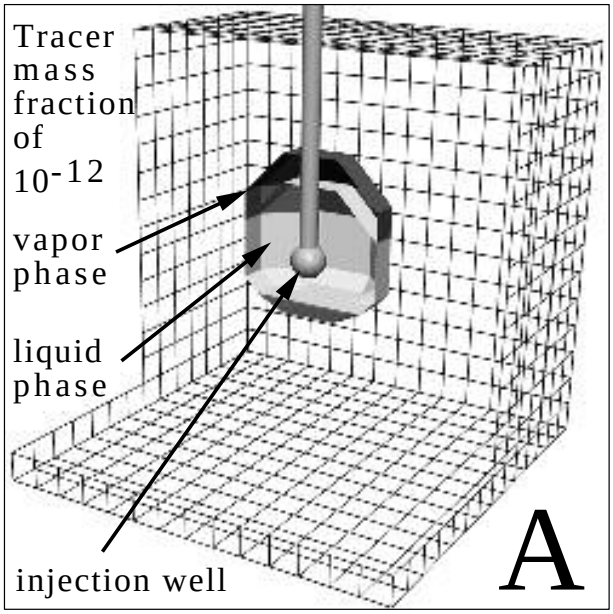
Tracer
mass
fraction
of
10-12
vapor
phase
liquid
phase
injection well
A

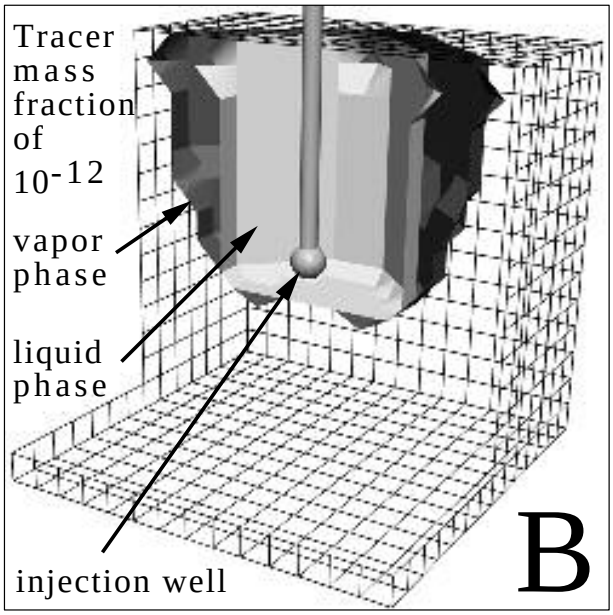
Tracer
mass
fraction
of
10-12
vapor
phase
liquid
phase
injection well
B

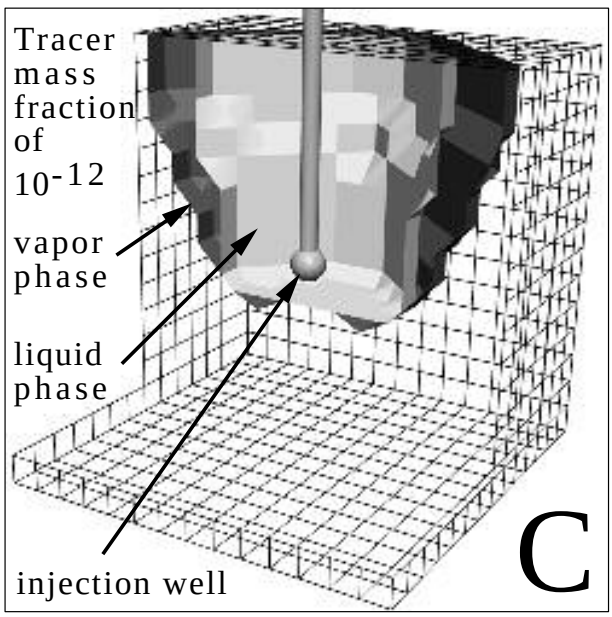
Tracer
mass
fraction
of
10-12
vapor
phase
liquid
phase
injection well
C

Compound	$M(\mathrm{kg/mol})$	$T^c(^\circ\mathrm{C})$	$P^c(\mathrm{MPa})$	ω	A^*	B^*	C^*
H_2O	0.018016	374	22.06	0.742	-	-	-
SF_6	0.146056	45.54	3.76	0.215	-42.0138	16.1840	30.0582
R-13	0.104459	28.81	3.946	0.180	-60.0736	11.1937	51.7480
R-14	0.088005	-45.65	3.739	0.186	-66.1391	4.7463	66.3009
R-22	0.086468	96.15	4.97	0.221	-56.3330	4.5208	53.9459
R-23	0.070014	25.74	4.836	0.267	-82.3196	8.7996	73.3207
R-116	0.138012	19.85	3.06	0.28	-79.9564	5.1976	79.3443
R-C318	0.200031	115.35	2.78	0.356	-86.7454	6.0113	84.0756
R-134a	0.102031	106.85	3.690	0.239	-59.0986	6.8705	54.0940
R-124	0.13648	126.75	3.72	0.281	-84.7575	8.5418	76.0311
R-125	0.120022	68.85	3.44	0.259	-127.7211	11.4972	112.2099

Nomenclature

A^*,B^*,C^*	correlation coefficients for the modified Harvey correlation
β	phase distribution coefficient for a gas tracer
C_H	standard state Henry's coefficient (Pa)
C_H^*	modified Henry's coefficient (Pa)
C_H^{expt}	experimentally calculated Henry's coefficient (Pa)
C_H^1	initial fit of experimental Henry's coefficient (Pa)
f	fugacity
$\hat{f}_i^k$	partial fugacity of component i in phase k
f_i	pure component fugacity of component i
f_i^s	pure component fugacity of component i at the standard pressure state
γ_i	liquid phase activity coefficient of component i
γ_{ij}	binary interaction coefficient between components i and j
M_i	molecular weight of component i ($\mathrm{kg/mol}$)
P_i	partial pressure of component i (Pa)
P_w^s	water vapor pressure (Pa)
P_i^c	critical pressure of pure component i (Pa)
$\hat{\phi}_i^k$	partial fugacity coefficient of component i in phase k
R	universal gas constant (8.314 $\mathrm{kJ/kmol.K}$)
ρ_i	density of component i ($\mathrm{kgm}^{\ 3}$)
T	temperature ($^\circ\mathrm{C}$)
T_a	absolute temperature (K)
T_i^c	critical temperature of pure component i ($^\circ\mathrm{C}$)
T_i^r	reduced temperature of component i, i.e. T_a/T_i^c
V	mixture molar volume ($\mathrm{m}^3\mathrm{mol}^{\ 1}$)
$\hat{V}_i^k$	partial molar volume at infinite dilution and standard pressure state for component i in phase k ($\mathrm{m}^3\mathrm{mol}^{\ 1}$)
w_i	acentric factor of component i
X_i	liquid phase mass fraction of component i
Y_i	vapor phase mass fraction of component i
x_i	liquid phase mole fraction of component i
y_i	vapor phase mole fraction of component i
Z	mixture compressibility